Engineering Research Express

PAPER

RECEIVED
10 September 2025

REVISED
16 December 2025

ACCEPTED FOR PUBLICATION
6 January 2026

PUBLISHED
19 January 2026

A multi-objective optimization of MQL milling parameters for aluminium alloy using biodegradable oil with fly ash additive

Ainusyafiqah Shaaroni[1], **Pay Jun Liew**[1,*], **Raja Izamshah Raja Abdullah**[1], **Kin Yuen Leong**[2] and **Jingsi Wang**[3]

[1] Fakulti Teknologi dan Kejuruteraan Industri dan Pembuatan, Universiti Teknikal Malaysia Melaka, Hang Tuah Jaya, 76100 Durian Tunggal, Melaka, Malaysia
[2] Department of Mechanical Engineering, Faculty of Engineering, Universiti Pertahanan Nasional Malaysia, Kem Sungai Besi, 57000, Kuala Lumpur, Malaysia
[3] Marine Engineering College, Dalian Maritime University, 1 Linghai Road, Ganjingzi District, Dalian 116026, People's Republic of China
[*] Author to whom any correspondence should be addressed.

E-mail: payjun@utem.edu.my

Keywords: fly ash, vegetable oils, minimum quantity lubrication, aluminium alloy, response surface methodology

Abstract

This study presents a multi-objective optimization of milling parameters for aluminium alloy under minimum quantity lubricant (MQL) conditions, employing biodegradable vegetable oil with and without the addition of fly ash. In this study, milling experiments were conducted based on a Response Surface Methodology (RSM) design of experiments. The effect of cutting speed, feed rate, depth of cut, and types of cutting fluid on the surface roughness (Ra), tool wear (Vb) , cutting force (Fc) and material removal rate (MRR) were investigated. Analysis of variance (ANOVA) was conducted to determine the significance of each parameter on machining performance. The findings indicated that the addition of fly ash to palm oil markedly enhanced surface quality and diminished tool wear. The machining performance improved by 33.8%, 70%, 19.8%, and 12.2% in terms of Ra, Vb, Fc, and MRR, respectively, when fly ash was added to palm oil compared to using palm oil alone. The optimal machining conditions for achieving the best multi-response outcomes were identified as a cutting speed of 3500 rpm, a feed rate of 840 mm min^{-1}, and a depth of cut of 1.0 mm.

1. Introduction

Nowdays, in manufacturing industry, there is an increasing demand for ecologically friendly and sustainable machining processes. Traditional cutting fluids are commonly used in machining processes to reduce friction, cool the workpiece, and remove chips [1, 2]. However, conventional cutting fluids offer remarkable environmental and health risks due to their chemical composition and disposal issues [3, 4]. To address these concerns, researchers have increasingly explored minimum quantity lubrication (MQL) as a viable alternative to conventional flood cooling during machining. MQL utilizes a minimal amount of lubricant, typically applied as a fine mist, thereby minimizing waste while maintaining effective lubrication. By directly applying the lubricant to the cutting zone, MQL reduces friction at the tool–workpiece interface and enhances surface finish [5, 6]. Numerous studies have demonstrated the efficacy of MQL in reducing tool wear and heat generation. However, the effectiveness of MQL strongly depends on the choice of lubricant and the optimization of cutting parameters, especially when machining aluminium alloys, which are prone to issues such as built-up edge (BUE) formation and thermal softening.

In this context, optimizing cutting parameters becomes essential for achieving desirable machining outcomes under MQL conditions. In milling, parameters such as cutting speed, feed rate, and depth of cut play a decisive role in determining surface quality, tool life, cutting force, and material removal rate (MRR) [7]. Higher cutting speeds generally enhance surface finish by reducing the contact time between tool and material. For example, Shokrani *et al* [8] found that greater cutting speeds resulted in smoother surfaces, with tool wear

decreased dramatically under dry cutting circumstances. Another notable example is the utilization of 3000 rpm spindle speed during milling of AA6061 aluminium alloy, where a MRR of 0.08 $mm^3\ s^{-1}$ was achieved with a feed of 0.05 mm $tooth^{-1}$ and depth of cut of 0.8 mm. This high-speed setup led to high productivity, producing a fine surface with Ra less than 1 μm, and effectively control tool wear [9]. However, unlike cutting speed, increasing the feed rate tends to have a trade-off. Although higher feed rates can enhance MRR, they often lead to a decline in surface quality due to greater scallop heights. Ikhries *et al* [10] found that machining 7075-T6 aluminium alloy at feed rates up to 750 mm min^{-1} significantly increased MRR but also raised Ra values. In addition to cutting speed and feed rate, depth of cut also affects tool wear and MRR, where larger depths elevate contact stress and flank wear. For instance, a depth of cut of 1.5 mm under dry conditions accelerated tool wear during milling aluminium alloy [11].

Beside cutting parameters, the choice of cutting fluid also gives a positive impact towards machining performance. In recent years, bio-based cutting fluids, particularly vegetable oils, have attracted attention as sustainable alternatives to conventional fluids due to their biodegradability, non-toxicity, and availability [12]. They have exceptional lubricating characteristics due to their intrinsic polarity and molecular structure [13]. Vegetable oils, such as sunflower oil, coconut oil, and palm oil, have strong lubricating properties in metal cutting processes. They are eco-friendly and offer superior lubrication compared to synthetic oils due to their high viscosity index and lubricity [14]. Selbmann *et al* [15] demonstrated that sunflower oil reduced cutting forces by 33%, and rapeseed oil improved tool wear and sustainability during the milling process. Similarly, in other applications, canola oil under MQL reduced tool wear by 33.3% and achieved excellent surface finishes [16]. To support sustainable machining goals, vegetable oils such as palm oil are also recognized for their natural biodegradability and low environmental impact, making them suitable for greener cutting fluid formulations [17].

To further enhance the performance of vegetable oils, researchers have incorporated nanoparticles to develop nanofluid-based MQL systems. Due to their unique thermal and tribological properties, these nanofluids help to reduce friction, improve heat dissipation, and extend tool life [18]. For example, by mixing alumina (Al_2O_3) nanoparticles into soybean oil, Minh *et al* [19] have demonstrated notable effectiveness in hard milling operations. Their study has showed remarkable reductions in tool wear and energy consumption due to enhanced lubrication and heat dissipation capabilities of the nanoparticles. Similarly, Zhenjing *et al* [9] investigated the effect of nanofluid-based MQL during milling of 7050 aluminium alloy by suspending Al_2O_3 nanoparticles into cottonseed oil. In addition to reducing cutting forces, the approach achieved a notable reduction in surface roughness to 0.087 μm representing a 30.4% improvement compared to conventional conditions. Meanwhile, Cönger *et al* [11] studied the use of vegetable oil enriched with molybdenum disulfide (MoS_2) nanoparticles for milling of Al6061-T651 aluminium alloy. Their result also showed significant improvements in machining performances. Specifically, they reported reductions of 74.2% in surface roughness, 63.9% in cutting force, and 27.9% in energy consumption compared to dry cutting conditions. Likewise, Gupta *et al* [20] compared mono and hybrid nanofluids during turning of stainless steel and reported that the hybrid suspension of Al_2O_3 and multi-walled carbon nanotubes (MWCNT) in soybean oil reduced tool flank wear by up to 11.35% compared to mononanofluid.

Although extensive research has been conducted on the various nanoparticle-enhanced cutting fluids in machining, the incorporation of solid waste-derived lubricants, particularly fly ash dispersed in vegetable oils remains largely unexplored. Fly ash, a fine particulate byproduct of coal combustion, possesses favorable thermal and tribological properties, including the ability to dissipate heat and reduce friction. Its natural constituents, such as silica (SiO_2) and Al_2O_3, further contribute to its suitability as a solid lubricant [21, 22]. Unlike commercial nanoparticle additives which are often expensive, fly ash offers a cost-effective and environmentally friendly alternative to MQL lubrication. Importantly, its incorporation into biodegradable, non-toxic and environmentally friendly vegetable oils such as palm oil provides a fully traceable, environmentally friendly coolant while eliminating the need for commercially synthesized nanoparticles.

The novelty of this work lies in introducing fly ash as an alternative solid lubricant in palm-oil-based MQL machining, a concept that has not been previously reported, and in systematically evaluating its performance relative to pure palm oil under identical conditions. This study evaluated the performance of the proposed cutting fluid during the machining of aluminium alloys by optimizing cutting parameters using response surface methodology (RSM) with Box-Behnken Design (BBD). Surface roughness, tool wear, cutting force, and MRR were simultaneously assessed to provide a comprehensive evaluation of lubrication efficiency. By transforming an industrial waste material into a value-added lubricant, this work contributes a novel, sustainable, and economically viable approach to green machining research.

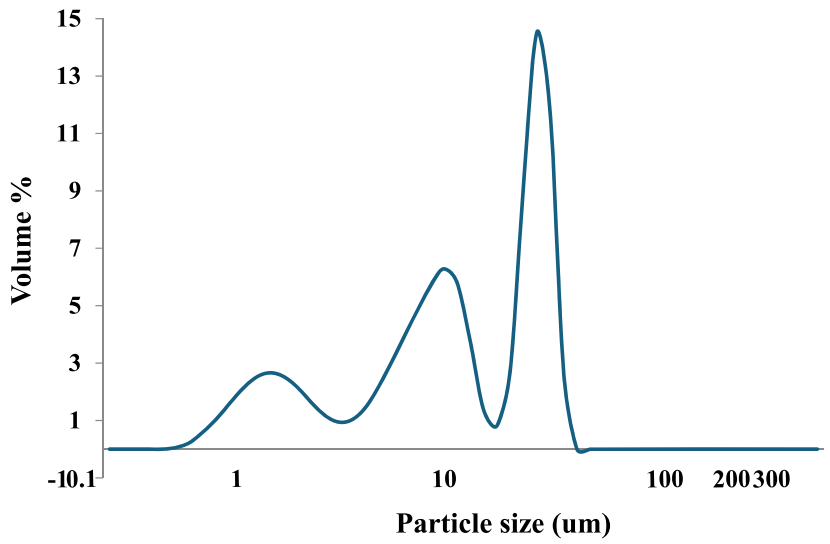

Figure 1. Particle size distribution of the sieved fly ash obtained using PSA.

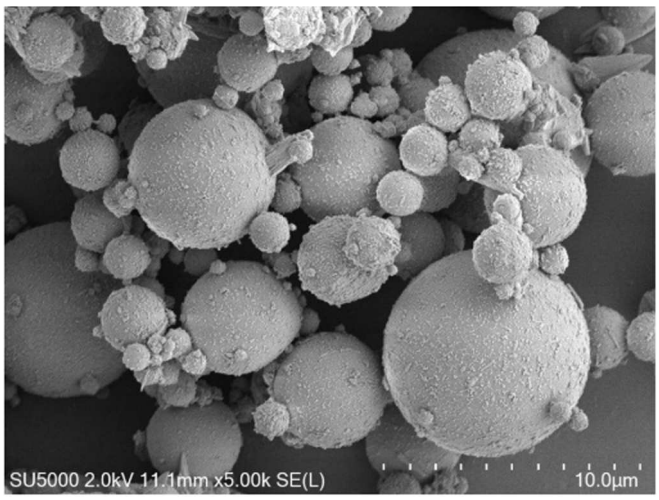

Figure 2. FESEM of fly ash.

2. Experimental method

2.1. Materials

The material selected for the machining process was aluminium alloy 6061. This alloy is widely used in aerospace and automotive applications due to its excellent mechanical properties and machinability [23]. The dimension of aluminium alloy used in this study was 45 × 100 × 15 mm (width × length × height).

The additives used in this study was fly ash, which obtained from the Jimah Power Plant in Port Dickson, Malaysia. The fresh fly ash was sieved using a 20 μm mesh to refine the particle size as the raw material exhibited relatively large particles averaging between 100 and 300 μm. The particle size distribution of the sieved fly ash was further verified using a Particle Size Analyzer (PSA), which confirmed an average particle size of approximately 13 μm (figure 1) ensuring that the particles were sufficiently fine for stable suspension in the palm oil base fluid. Figure 2 shows the micrograph of fly ash using field emission scanning electron microscope (FESEM). Table 1 shows the material composition of fly ash, which was obtained using the x-ray fluorescence (XRF) analysis. As can be seen from table 1, the main elements are SiO_2 (63.5%), Fe_2O_3 (17.06%), Cao (6%) and Al_2O_3 (5.2%), with the remaining composition made up of other elements. This fly ash can be classified as Class F, as the total composition of SiO_2, Fe_2O_3, and Al_2O_3 is 85.76%, exceeding the 70% requirement for this classification.

Table 1. Material composition of fly ash (%) obtained through XRF analysis.

SiO_2	Fe_2O_3	CaO	Al_2O_3	K_2O	SO_3	BaO	Other elements
63.50	17.06	6.00	5.20	2.64	2.43	1.09	2.08

2.2. Preparation and properties of fly ash suspension

In this study, pure palm oil was served as the base fluid because of its inherent biodegradability and non-toxic properties, making it more ecologically friendly than traditional mineral oils. The use of fly ash, an industrial waste material, further enhances the sustainability of the formulation by eliminating the need for chemically synthesized additives. As a result, the formulated cutting fluid aligns with the study's objective of producing a biodegradable and eco-friendly lubrication system.

Before the machining, a fly ash suspension was prepared by dispersing fly ash particles into pure palm oil at a concentration of 2 wt% by using equation (1). The mixture was produced using a two-step method [24]. In the first step, surfactant which is sodium dodecyl sulphate (SDS) was mixed into palm oil using an ultrasonic homogenizer for 15 min. Subsequently, the fly ash particles were dispersed into the mixture for an additional 30 min. The surfactant was added into the solution to ensure the stability of the suspension [25]. Throughout the ultrasonic process, the sample was immersed in cold water to prevent any temperature rise. The titanium probe with a diameter of 14 mm was used to transmit vibrations, which was suitable for processing sample volumes ranging from 100 to 2000 ml.

$$\text{Weight\%} = \frac{\text{mass of solution}}{\text{mass of solute}} \times 100 \tag{1}$$

To ensure the stability of the fly ash suspension, the solution was observed immediately after sonication, as well as after one hour, one day, and one week. The results of these observations are summarized in figure 3. Initially, both fly ash mixtures (with and without surfactant) were well-dispersed in the base fluid. However, the suspension prepared without surfactant exhibited rapid particle settling after one day (figure 3(c)), with the fly ash beginning to sediment at the bottom of the bottle. After one week, the fly ash was completely settled, leaving the palm oil clear (figure 3(d)) . In contrast, the addition of SDS significantly enhanced dispersion, producing a more stable and uniform suspension and only start to sediment after one week. These findings confirm the effectiveness of the surfactant in maintaining consistent particle distribution during machining. Furthermore, to ensure uniform dispersion before each machining trial, the fly ash–palm oil mixture was homogenized for 15 min in an ultrasonic bath prior to use, preventing sedimentation or particle agglomeration before the fluid was supplied through the MQL system.

The thermo-physical behaviour of the formulated cutting fluid was characterised to support the analysis of lubrication and heat-transfer performance. Dynamic viscosity of the fly ash suspension was measured by a rotational-type HAAKE Viscometer 2 with a measurement range of 0.3–10 000 mPas. The sample was heated on a magnetic hot plate to reach the desired temperatures, and viscosity was recorded at 30 °C, 40 °C, 50 °C, and 60 °C. As shown in figure 4, consistent with typical vegetable-oil-based lubricants, the fly ash suspension viscosity decreases with increasing temperature, thereby improving fluid atomization and penetration at the tool–chip interface during high-speed machining.

The thermal conductivity of the fly ash suspension was measured using a Linseis THB500 thermal conductivity analyser. The mixture was placed inside the instrument chamber, and a heated wire probe was immersed in the sample. The transient temperature rise over time was used to determine thermal conductivity at 25 °C, 30 °C, 35 °C, and 40 °C. As can be seen in figure 5, thermal conductivity increases with temperature, indicating enhanced heat dissipation, which is beneficial for reducing thermal load and tool-workpiece adhesion during MQL milling.

2.3. Machining process

The machining experiments were carried out using CNC milling machine (HAAS VOP-C). A carbide insert of type APET103504PDFR-S (H1 grade) from Sumitomo, designed specifically for aluminium alloys was used in the present work and mounted on E90AP10-D20 tool holder. The machining experiments were performed using two cutting fluid conditions: (1) pure palm oil and (2) palm oil with 2 wt% suspended fly ash. MQL conditions were kept constant during the milling experiments. MQL was applied via a micro-droplet nozzle that delivered lubrication in the form of oil mist. The experiments were performed under normal laboratory ambient conditions. While, the cutting fluid flow rate was determined using a volumetric method, where the amount of fluid discharged over a fixed period was measured to ensure a consistent delivery rate of approximately 1.5 ml min^{-1} to ensure precise cutting fluid delivery to the cutting zone. Meanwhile, the air supply was maintained at the machine's regulated default pressure. The nozzle was mounted approximately

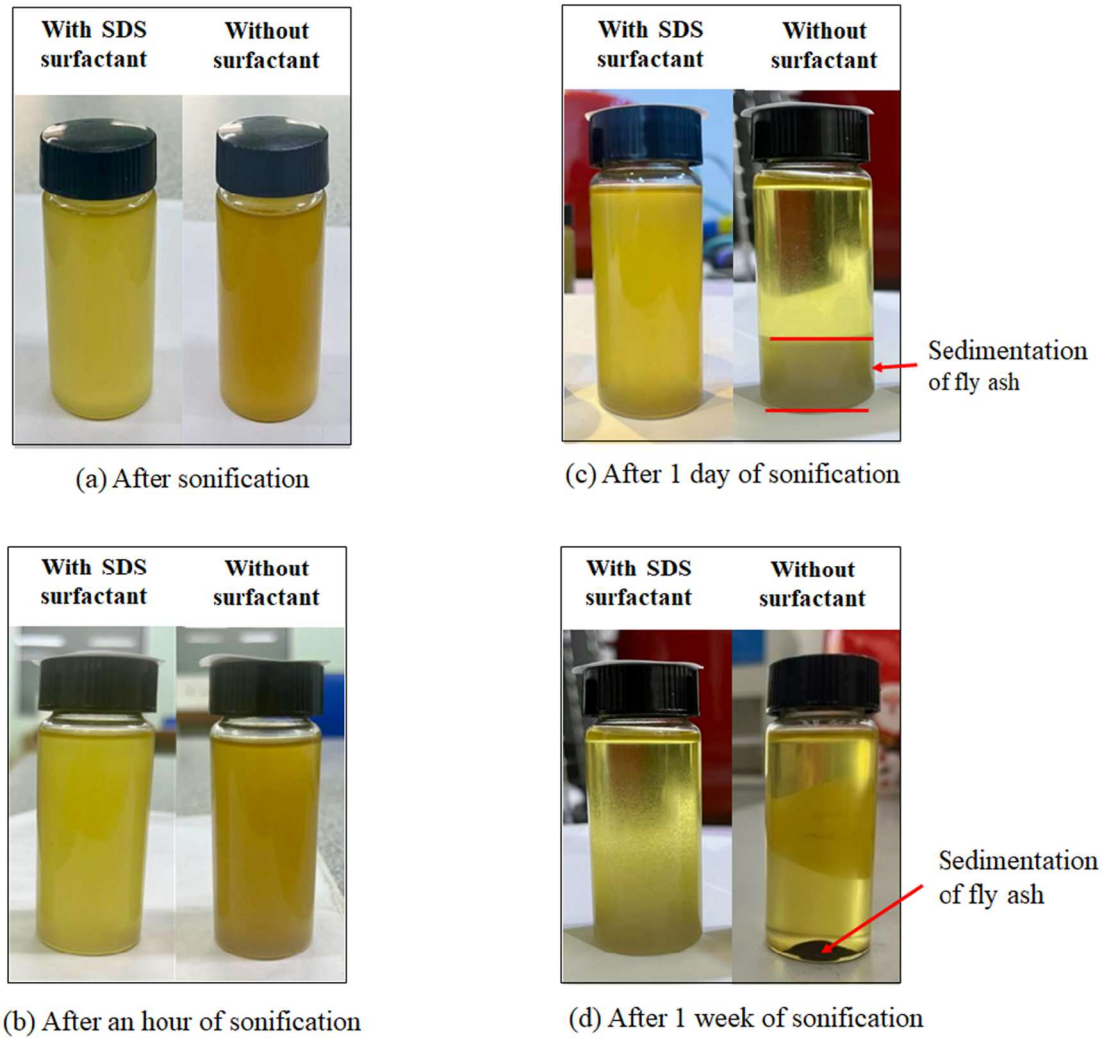

Figure 3. Fly ash suspension observation.

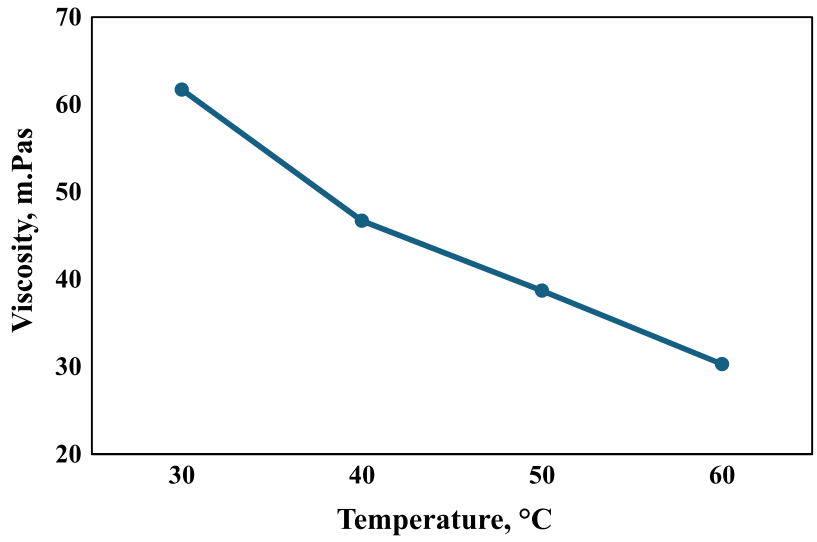

Figure 4. Viscosity plots against temperature.

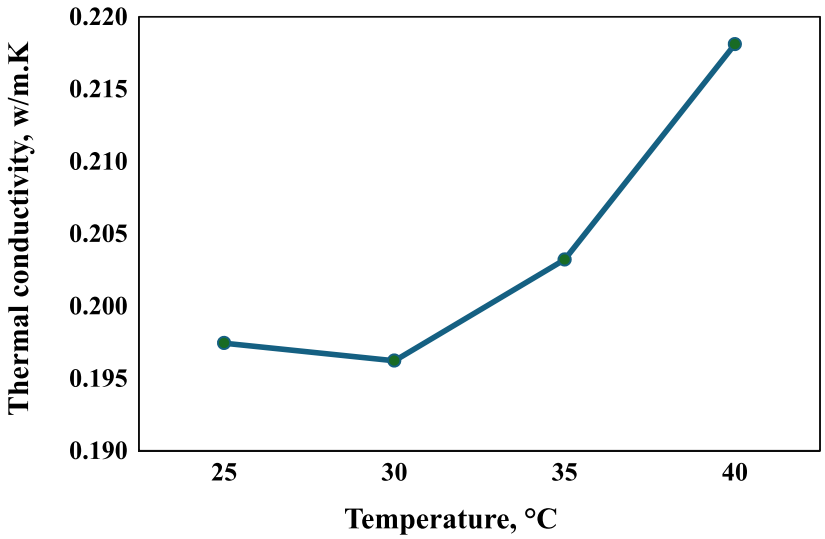

Figure 5. Thermal conductivity plots against temperature.

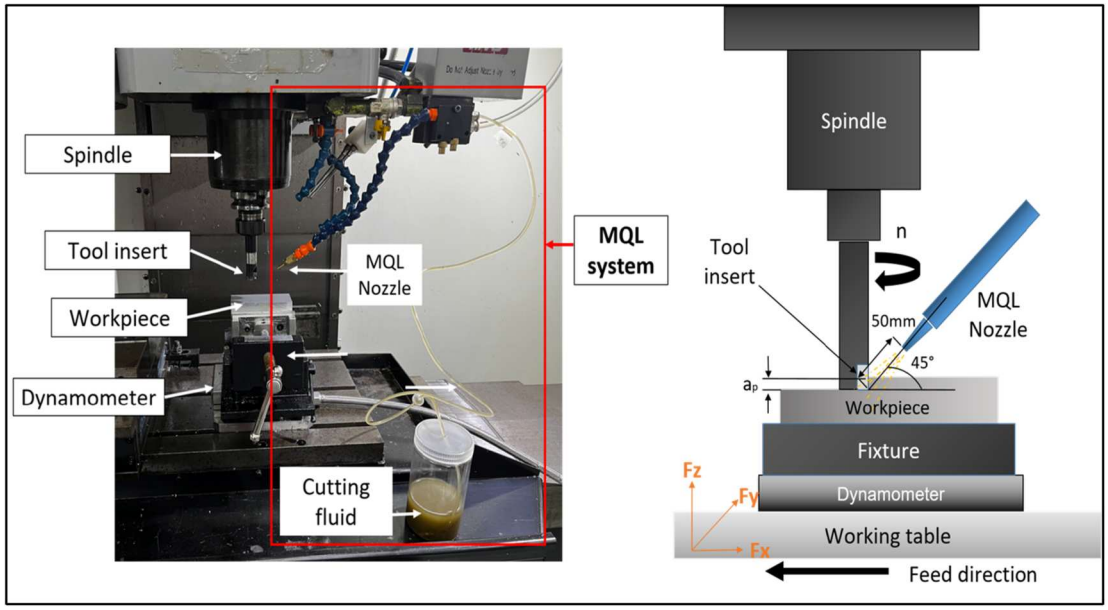

Figure 6. Experimental setup of milling process.

50 mm from the cutting zone at an inclination angle of about 45° to ensure effective impingement of the spray at the tool–workpiece interface. The experimental setup is shown in figure 6.

2.4. Measurement and analysis

To evaluate machining performances, surface roughness, tool wear, cutting force and MRR were measured. Surface roughness measurements were conducted using a Mitutoyo portable surface roughness tester (cutoff length: 0.8 mm) in accordance with ISO 4287 standards. Nine measurements were taken along each machined surface, from which the average Ra value was calculated. Meanwhile, the tool wear was measured by using a Mitutoyo tool-maker microscope. The admissible flank wear was measured at the flank area (Vb) according to the ISO 3685 standard (1993). The Ra and Vb values were taken after 3500 mm tool travel for each run.

Simultaneously, cutting force measurement was done using dynamometers that capture forces acting on the tool–workpiece system. MRR was measured based on the weight difference of the workpiece before and after machining. A precision digital balance was used to record the initial and final weights, while the machining time was tracked using a digital stopwatch. All measurements were taken consistently after the tool had travelled a distance of 3500 mm for each experimental run.

Table 2. Cutting parameters for milling process.

Cutting parameter	Level 1	Level 2	Level 3
Cutting speed (rpm)	1500	2500	3500
Feed rate (mm/min)	400	700	1000
Depth of cut (mm)	0.5	0.8	1.0
Type of cutting fluid	Palm oil	Fly ash suspension	

2.5. Design of experiment

Design of Experiments (DoE) has become an important method in machining research, particularly for improving milling operations. In this work, the RSM with a BBD was used to explore the effects of type of cutting fluid, cutting speed, feed rate and depth of cut on surface roughness, tool wear, cutting force and MRR during milling of aluminium 6061. Among the numerous DoE methodologies, RSM has proven especially beneficial for modeling complicated connections. The BBD is a highly effective and popular RSM-based design. This approach was chosen due to its ability to model factor interactions and optimize multiple responses with minimal experimental runs [26–28]. The experimental design incorporated three numerical parameters (cutting speed, feed rate, and depth of cut) at three levels each, along with one categorical variable (type of cutting fluid) with two distinct levels, as shown in table 2. The machining parameter ranges were selected based on a combination of tool manufacturer's recommendations for carbide end mills used in machining aluminium alloys, insights from previous studies on MQL milling of AL6061-T6, and preliminary trial cuts conducted in this study.

In the RSM, the relationship between input parameters and output responses was modeled using a second-order polynomial equation, enabling evaluation of both linear and interaction effects. ANOVA was conducted to determine the statistical significance of each parameter and their interactions. All statistical analyses were performed using Design-Expert software.. In this study, the centre points which function as internal replications for estimating pure error, were defined at the mid-levels of all numerical factors. Because a categorical factor (type of cutting fluid) was included, these numerical centre-point runs were replicated three times within each coolant category, providing sufficient pure error estimation and allowing curvature detection across the numerical design space. Subsequently, regression analysis and response surface plots were employed to visualize relationships and identify optimal parameter combinations.

3. Results and discussions

The experimental data was analyzed using Design-Expert software to evaluate individual factor effects on response variables and generate predictive models. The results for the Ra, Vb, Fc and MRR are presented sequentially, with corresponding experimental data detailed in table 3.

3.1. Surface roughness

After removing the insignificant factors, the ANOVA for surface roughness in terms of the independent variable is shown in table 4. From the ANOVA analysis, a model F-value of 16.93 implies that the model is significant. The critical F-value for a significance level of $\alpha = 0.05$ with degree of freedoms $df_1 = 4$ and $df_2 = 25$ is approximately 2.76, as obtained from F-distribution table [29]. Since the calculated model F-value (16.93) is far greater than this value, the model is statistically significant at the 95% confidence level. There is less than 0.01% chance that a 'Model F- Value' this large could occur due to noise. The values of p (Prob > F) were also less than 0.05 indicating that the model terms are significant with 95% confidence level. Physically, the high F-value indicates a strong signal-to-noise ratio between the modelled variance and the residual variance, thereby confirming that the selected cutting parameters significantly affect surface roughness. Therefore, in this investigation, all factors were identified as significant model terms.

Table 5 summarizes the statistical performance of the developed Ra model. The determination coefficient, $R^2 = 0.7303$, means that 73.03% of the variation in surface roughness is explained by the selected process parameters. The adjusted $R^2 = 0.6872$, considering the number of model terms, is close to the R^2 value, and therefore, the model is not over-fitted. The predicted $R^2 = 0.6035$ is in reasonable agreement with the adjusted R^2, which means the model is fairly adequate to predict the variation in the experimental design. Also, the Adeq Precision of 15.0620, much greater than the recommended threshold value of 4, strongly indicates an adequate signal-to-noise ratio, which confirms that the model is sufficiently accurate to describe the navigation of the design space.

Table 3. Experimental result of the milling of aluminium 6061.

Std	A: cutting speed, rpm	B: feed rate, mm/min	C: depth of cut, mm	D: type of coolant	Ra, μm	Vb, mm	Fc, N	MRR, mm^3/min
1	1500	400	0.8	Palm oil	1.111	0.146	55.620	2222.2
2	3500	400	0.8	Palm oil	0.443	0.019	78.540	2244.4
3	1500	1000	0.8	Palm oil	1.825	1.621	59.180	5022.2
4	3500	1000	0.8	Palm oil	1.269	0.017	36.447	5088.9
5	1500	700	0.5	Palm oil	0.857	0.013	21.474	2377.8
6	3500	700	0.5	Palm oil	0.859	0.017	28.161	2444.4
7	1500	700	1.0	Palm oil	1.607	1.694	48.129	4466.7
8	3500	700	1.0	Palm oil	0.837	0.016	85.255	4755.6
9	2500	400	0.5	Palm oil	0.714	0.020	47.959	1377.8
10	2500	1000	0.5	Palm oil	0.877	0.718	31.426	2844.4
11	2500	400	1.0	Palm oil	0.720	0.009	73.530	2800.0
12	2500	1000	1.0	Palm oil	1.027	1.745	56.467	4644.4
13	2500	700	0.8	Palm oil	1.254	0.114	43.223	3600.0
14	2500	700	0.8	Palm oil	1.207	0.183	45.319	3888.9
15	2500	700	0.8	Palm oil	1.004	0.831	49.298	3688.9
16	1500	400	0.8	Fly ash suspension	0.550	0.039	34.710	2400.0
17	3500	400	0.8	Fly ash suspension	0.380	0.047	45.266	2400.0
18	1500	1000	0.8	Fly ash suspension	1.279	0.017	24.602	6200.0
19	3500	1000	0.8	Fly ash suspension	0.841	0.062	32.450	4800.0
20	1500	700	0.5	Fly ash suspension	0.671	0.008	53.837	3111.1
21	3500	700	0.5	Fly ash suspension	0.190	0.043	38.200	3844.4
22	1500	700	1.0	Fly ash suspension	1.087	0.755	37.700	4511.1
23	3500	700	1.0	Fly ash suspension	0.728	0.047	35.986	3111.1
24	2500	400	0.5	Fly ash suspension	0.659	0.007	50.160	1488.9
25	2500	1000	0.5	Fly ash suspension	0.754	0.010	53.950	5577.8
26	2500	400	1.0	Fly ash suspension	0.596	0.018	32.540	2600.0
27	2500	1000	1.0	Fly ash suspension	0.961	0.994	38.530	6177.8
28	2500	700	0.8	Fly ash suspension	0.624	0.026	37.810	3577.8
29	2500	700	0.8	Fly ash suspension	0.597	0.032	39.857	4333.3
30	2500	700	0.8	Fly ash suspension	0.420	0.039	54.320	3622.2

Table 4. ANOVA for surface roughness.

Source	Sum of squares	df	Mean square	F-value	p-value
Model	2.75	4	0.6874	16.93	<0.0001
A-Cutting Speed	0.7396	1	0.7396	18.21	0.0002
B-Feed Rate	0.8372	1	0.8372	20.62	0.0001
C-Depth of Cut	0.2455	1	0.2455	6.05	0.0212
D-Type of cutting fluid	0.9272	1	0.9272	22.83	<0.0001
Residual	1.02	25	0.0406		
Lack of Fit	0.9553	21	0.0455	3.04	0.1447
Pure Error	0.0599	4	0.0150		
Cor Total	3.76	29			

Table 5. Statistical summary of model for Ra.

R^2	Adjusted R^2	Predicted R^2	Adeq precision
0.7303	0.6872	0.6035	15.0620

The Ra prediction models were developed through regression analysis. These machinability models can be used to predict the Ra value at any point within the selected range of process parameters by substituting the values into equation (2).

$$Ra = 0.86493333333333 - 0.215A + 0.22875B + 0.123875C - 0.1758D \quad (2)$$

Figure 7 shows the normal probability plot of residuals. This plot is employed to assess the normality assumption for the ANOVA model. The residuals are in close proximity to the straight reference line, thereby

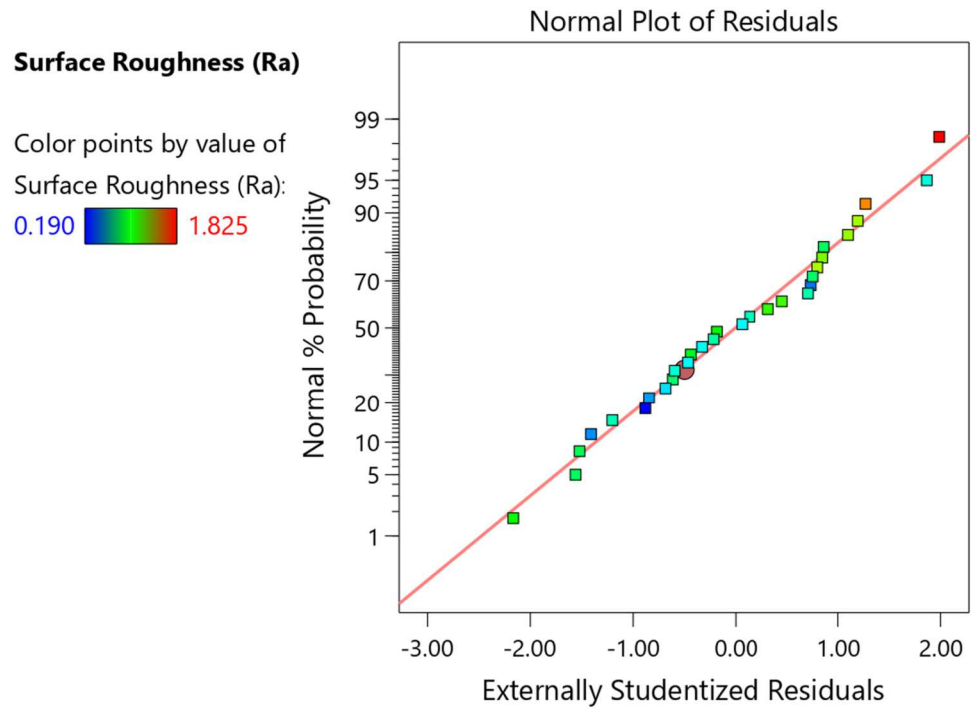

Figure 7. Normal probability plot for surface roughness.

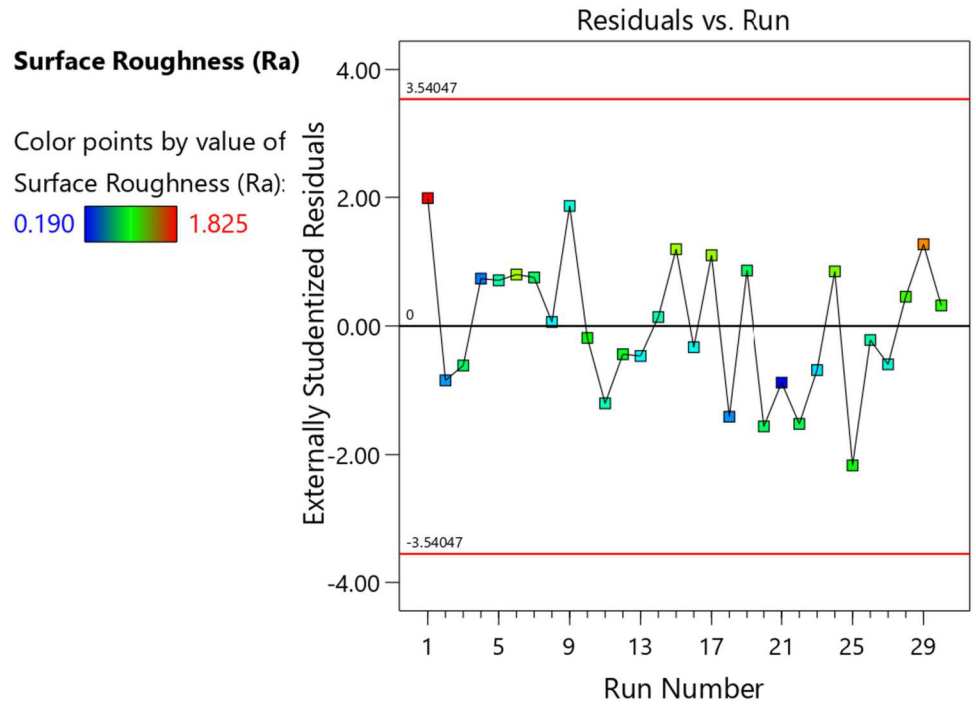

Figure 8. Residuals versus run for surface roughness.

supporting the notion that the errors are normally distributed consistent with the recommendations made by Montgomery [29]. Figure 8 highlights the externally studentized residuals, which will be employed to detect the presence of suspected outliers or influential points. The residuals-versus-run plot indicates no identified trend or drift, supporting the independence of observations and satisfying the requirements set forth by Anderson and Whitcomb [30]. Meanwhile, figure 9 depicts residuals versus the predicted values of surface roughness. It can be identified that data presents a random trend without any definite pattern that signifies the satisfaction of

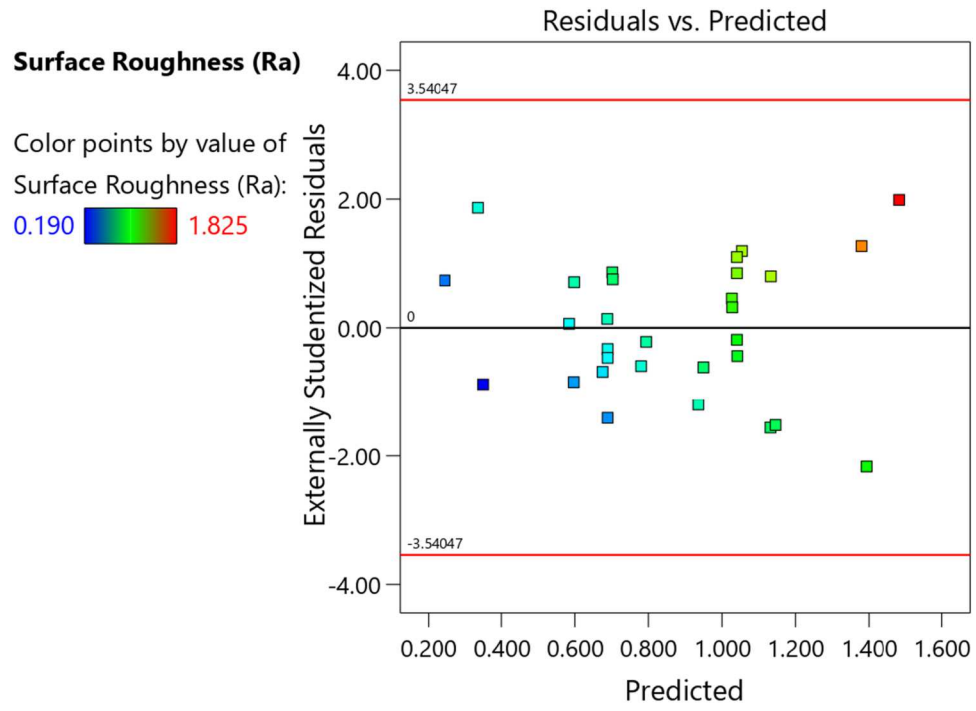

Figure 9. Residuals versus predicted values for surface roughness.

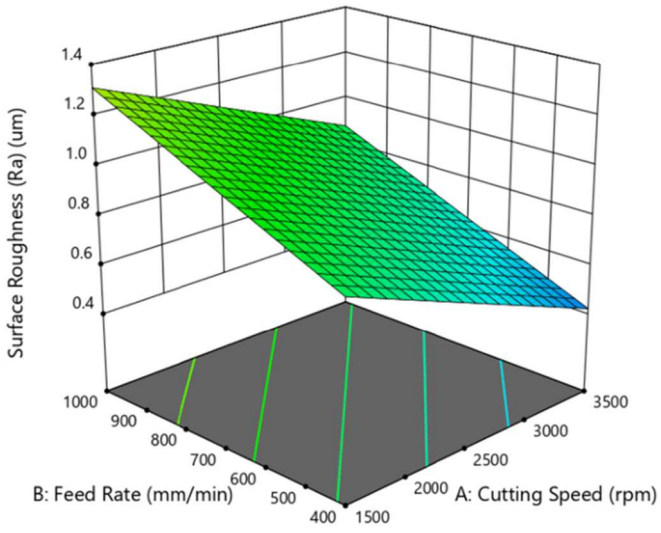

Figure 10. Response surface plot which showing the interaction between feed rate and cutting speed on Ra.

model adequacy and constant variance criteria. The top and lower red lines represent the Bonferroni-adjusted control limits for externally studentized residuals (±3.54047). Since all points fall inside these limits, no data point can be regarded as an outlier or an extreme observation. Overall, these diagnostics confirm that the Ra model satisfies the basic ANOVA assumptions.

Figure 10 depicts the response surface plot for the interaction between feed rate and cutting speed on Ra. From the figure, it shows that the optimal surface finish was found at higher cutting speed and lower feed rate. These results are similar to the findings of Jayakumar [26], who observed that this trend is due to the combined thermal and mechanical effects of machining. At greater cutting speeds, the process may become more adiabatic, restricting heat dissipation and resulting in localized temperature increases. This softens the material, promotes grain boundary movement, and lowers cutting pressures, resulting in a smoother surface finish. Meanwhile, lower feed rates may reduce tool marks by minimizing the amount of material removed every revolution, which enhances surface quality.

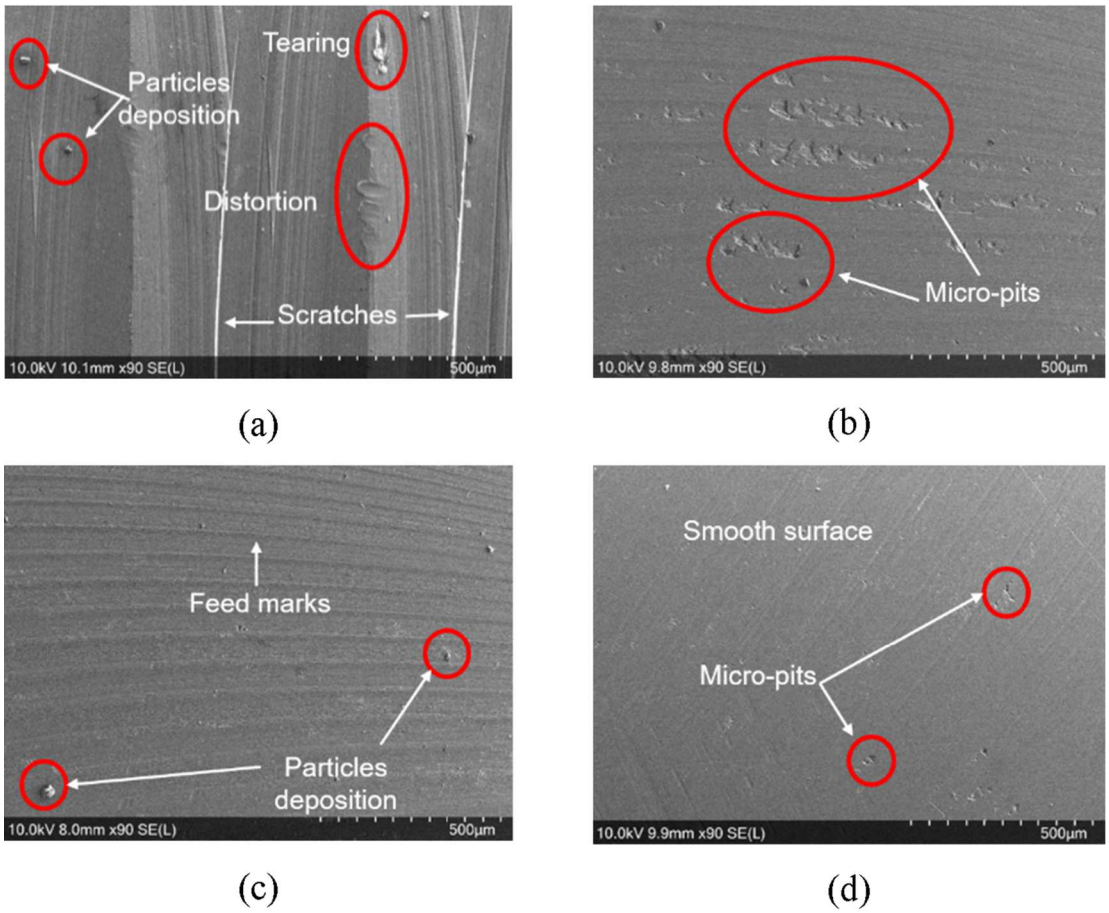

Figure 11. FESEM images of workpiece surface under different working condition (a) Run 1 (Std 3) (b) Run 23 (Std 28) (c) Run 9 (Std 6), (d) Run 26 (Std 21).

To further evaluate the surface finish of the machined samples, FESEM observations were conducted, as shown in figure 11. In figure 11(a), Run 1 which conducted at 1500 rpm cutting speed, 1000 mm min^{-1} feed rate, and 0.8 mm depth of cut using pure palm oil, produced the most severe surface damage, with the highest roughness value of 1.825 µm. Severe machining marks such as deep scratches, tearing, distortion, and particle deposition were clearly observed. This rough surface quality can be attributed to the combination of a relatively low cutting speed and high feed rate, which increased tool–workpiece interaction forces and led to higher friction and heat generation during milling [31].

In contrast, figure 11(b) presents the surface machined at a higher cutting speed of 2500 rpm and a reduced feed rate of 700 mm min^{-1}, with the same depth of cut (0.8 mm) but employing fly ash suspension as cutting fluid. The surface morphology improved significantly, exhibiting more uniform polishing lines and fewer severe defects compared to figure 11(a). The introduction of fly ash particles into the cutting fluid likely enhanced lubrication at the tool–chip interface, thereby reducing friction. However, a considerable number of micro-pits were still observed. suggesting particle entrapment between the tool and workpiece, where repeated impacts may initiated localized stresses and surface damages [32].

Figure 11(c) shows the surface obtained at an even higher cutting speed of 3500 rpm, with a feed rate of 700 mm min^{-1} and a reduced depth of cut (0.5 mm), using only palm oil as the cutting fluid. The surface exhibited a smoother texture with visible but shallow feed marks and minimal particle deposition. The combination of increased cutting speed and reduced depth of cut effectively lowered cutting forces and thermal input, thereby enhancing the surface quality compared to those observed in figures 11(a) and (b).

However, the machined surface in figure 11(d), produced under the same cutting parameters as figure 11(c) but with fly ash suspension as the cutting fluid, exhibited the best overall surface quality, characterized by a smooth texture ($Ra < 0.2$ µm), minimal defects, and markedly reduced micro-pit formation. The incorporation of fly ash into palm oil formed a protective tribo-film on the tool–workpiece interface, which reduced friction, heat generation, and adhesion. Besides that, the spherical shape of the alumina and silica particles in fly ash enables a micro-polishing effect, which contributes to a finer and smoother machined surface. As a result, material removal was more stable, leading to superior surface integrity. These findings are aligned with the

Table 6. ANOVA for tool wear.

Source	Sum of squares	df	Mean square	F-value	p-value
Model	61.34	6	10.22	7.38	0.0002
A-Cutting Speed	7.08	1	7.08	5.12	0.0334
B-Feed Rate	13.99	1	13.99	10.10	0.0042
C-Depth of Cut	14.29	1	14.29	10.32	0.0039
D-Type of cutting fluid	6.94	1	6.94	5.01	0.0351
AC	10.92	1	10.92	7.89	0.0100
AD	8.11	1	8.11	5.86	0.0238
Residual	31.84	23	1.38		
Lack of Fit	29.60	19	1.56	2.78	0.1658
Pure Error	2.24	4	0.5601		
Cor Total	93.17	29			

Table 7. Statistical summary of model for Vb.

R^2	Adjusted R^2	Predicted R^2	Adeq precision
0.6586	0.5695	0.4284	11.6790

observation of Zadafiya *et al* [33] where they established understanding that both lubrication effectiveness and optimized machining parameters significantly influence surface integrity during metal cutting processes.

Across the tested cutting conditions, the addition of fly ash reduced surface roughness by up to 33.8% compared to that of pure palm oil, confirming its strong ability to improve surface integrity. This improvement can be attributed to the presence of fine SiO_2 and Al_2O_3 particles in fly ash, which strengthen the lubricating film and reduce friction at the tool–workpiece interface. The reduction in surface roughness obtained using fly-ash-based palm oil is in agreement with the previous reports on particle-enhanced MQL lubricants. The nano-silica additives in Sen *et al* [21] resulted in marked improvement in the machined surface owing to superior heat dissipation and improved lubrication. This indicates that even waste-derived fly ash can provide surface quality improvements comparable to engineered nano-particles.

3.2. Tool wear

Table 6 shows the ANOVA for the tool wear. Since the raw tool wear data exhibited non-constant variance, a natural logarithm transformation was applied to stabilise the variance and improve the model fit prior to ANOVA analysis. As shown in table 6, the Model F-value of 7.38 implies the model for ln(Vb) is statiscally significant. According to the F-distribution table [29] for $\alpha = 0.05$ with degrees of freedom $df_1 = 6$ and $df_2 = 23$, the critical F-value is approximately 2.53. Since the calculated value of 7.38 is much greater than this threshold, the likelihood of the model being significant due to random noise is very low. Parameter A, B, C, D and interaction of AC and AD are considered as significant model terms due to their p-value lower than 0.05.

The statistical indicators for the tool wear model are presented in table 7. The R^2 value of 0.6586 implies that the regression model explains 65.86% of the variation in tool wear using the chosen cutting parameters. The adjusted R^2 of 0.5695 remains reasonably close to the R^2; hence, the model does not appear over-fitted. The predicted R^2 of 0.4284 is in acceptable agreement with the adjusted R^2, with a difference less than 0.2, implying a moderate predictive capability. The signal-to-noise ratio in the Adeq. Precision value of 11.6790 is greater than the recommended minimum value of 4, indicating that the model can be reliably.

Based upon the proposed second-order polynomial model, the effects of the process parameter on tool wear can be calculated by computing the values of the different constants of equation (3).

$$\ln(\mathrm{Vb}) = -2.75 - 0.6654\,\mathrm{A} + 0.9349\,\mathrm{B} + 0.9450\mathrm{C} - 0.4810\,\mathrm{D} - 1.17\,\mathrm{AC} + 0.7122\,\mathrm{AD} \quad (3)$$

Figures 12 to 14 depict residual diagnostic plots for tool wear. The normal probability plot (figure 12) indicates that most residual points lie close to the reference line, ensuring that residuals are normally distributed. The residuals-versus-run plot (figure 13) does not show any trending behavior; this means there is independence of errors within the experimental sequence. In the residuals-versus-predicted plot (figure 14), the points

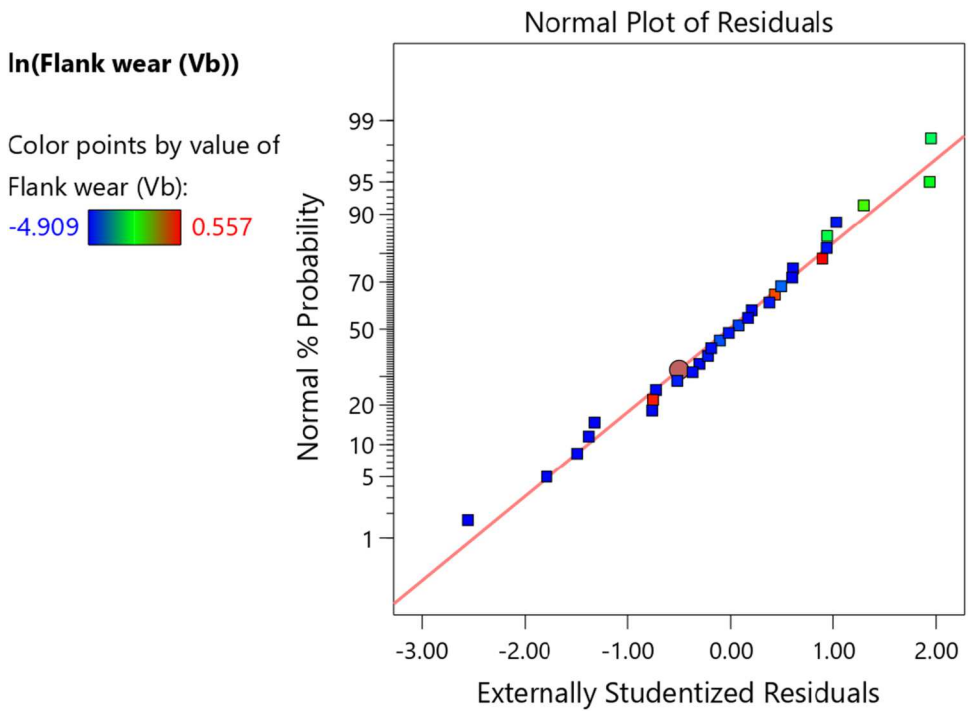

Figure 12. Normal probability plot for tool wear.

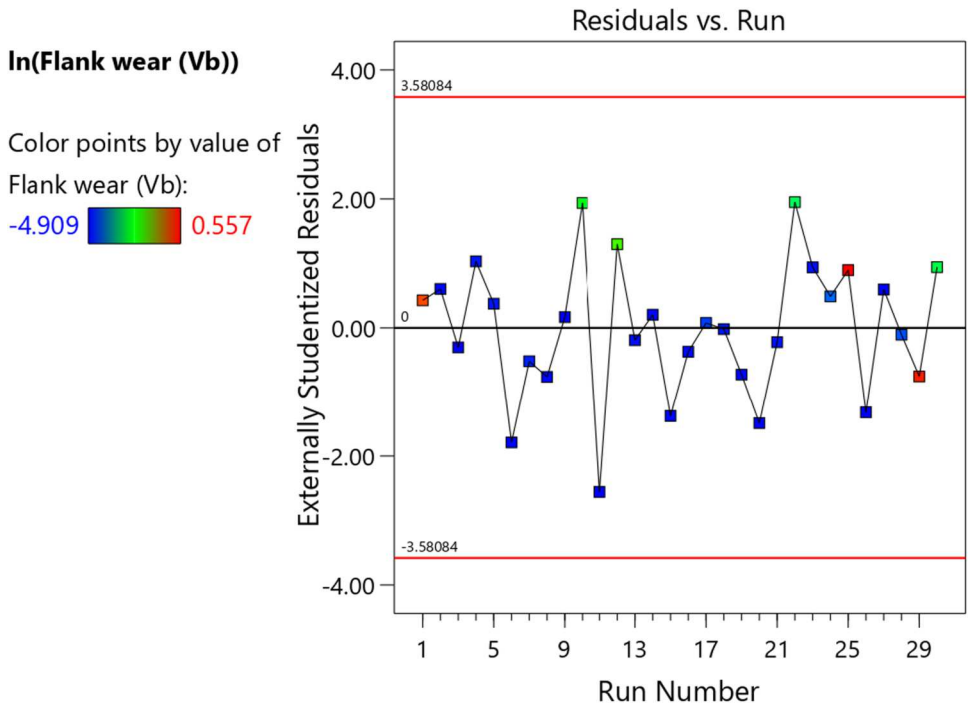

Figure 13. Residuals versus run for tool wear.

scatter uniformly around the zero-residual axis, indicating constant variability across the range of fitted values and hence satisfying homoscedasticity. The externally studentized residual limits, at ± 3.58084, indicate that none of the observations exceed the outlier boundaries, hence confirming the integrity of the tool wear data for further modeling.

Figure 15(a) shows the interaction plot between cutting speed and depth of cut on tool wear. When the depth of cut is low, tool wear remains consistently low across the range of cutting speed, indicating that the tool can withstand lower mechanical loads without notable degradation. However, when the depth of cut is raised to

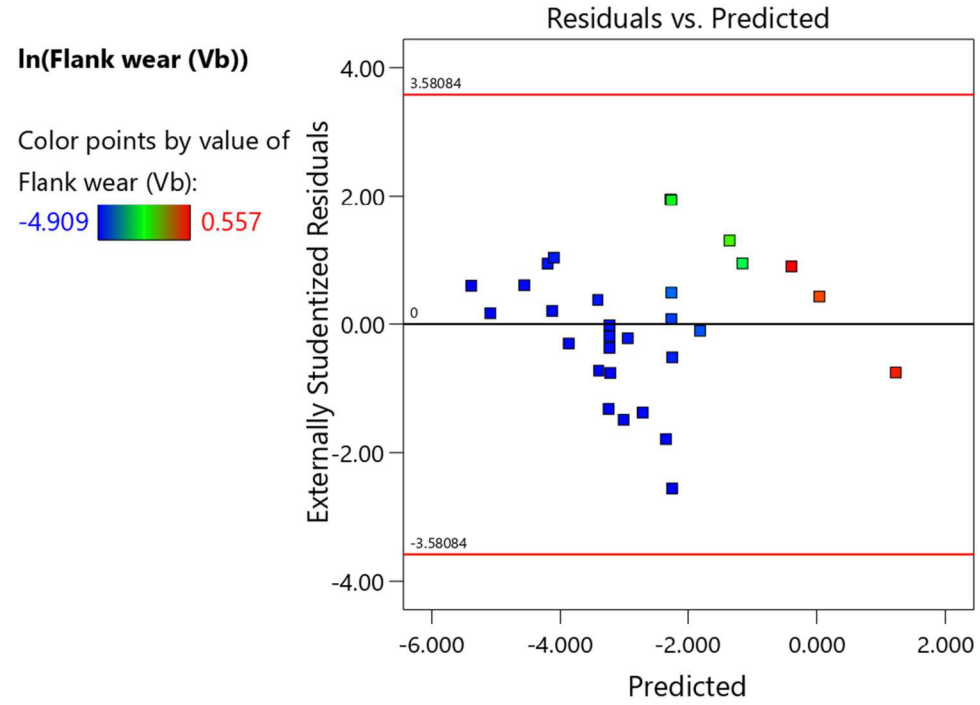

Figure 14. Residuals versus predicted values for tool wear.

1.0 mm, tool wear increases considerably, especially at lower cutting speeds. As the cutting speed surpasses 2000 rpm, tool wear decreases sharply. This trend can be attributed to two competing mechanisms where at low cutting speeds and greater depths of cut, mechanical stresses and friction predominate, leading to severe abrasive and adhesive wear [34]. The decrease in tool wear with increasing cutting speed can be attributed to the reduced chip–tool contact time per engagement. Although the total machining distance was kept constant for all runs, higher cutting speeds shorten the interaction duration between the tool and the workpiece. This reduced contact time suppresses adhesion and built-up-edge formation, promoting smoother chip evacuation and consequently lowering flank wear [35]. The cutting force results at 3500 rpm further support this trend, as Fc generally decreased with increasing speed, indicating reduced mechanical and frictional loading on the tool flank. Meanwhile, figure 15(b) compares the impact of the types of cutting fluid and cutting speed on tool wear. It is clear that fly ash suspension consistently reduces tool wear compared to palm oil across the entire cutting speed range. This shows that the functional additives improve lubrication, reduce friction, and generate protective boundary coatings, all of which help to reduce tool wear [36]. As can be seen from the figure, at higher cutting speeds, the difference between the two cutting fluids is minimal; but, at lower cutting speeds, the difference becomes more evident, with palm oil resulting in greater tool wear. This suggests that fly ash suspension possesses higher thermal stability and maintains its protective characteristics at elevated temperatures, whereas pure palm oil may breakdown or evaporate more quickly, losing its efficacy under high thermal loads.

Figure 16 presents the response surface plot for the interaction between cutting speed and feed rate on tool wear under different cutting fluids and depth of cut conditions. As indicated in figures 16(a) and (b), the surface maps are nearly flat, indicating low tool wear across the tested ranges of cutting speed and feed rate. This implies that the tool exhibits minimal wear at the lower depth of cut of 0.5 mm, regardless of the type of cutting fluid used. The combination of low mechanical stress and adequate lubrication at this cutting setting inhibits abrasive and adhesive wear processes, resulting in a longer tool life. Additionally, the slightly decreased wear observed with the fly ash suspension compared to pure palm oil suggests that the fly ash suspension provides enhanced protection to the cutting insert, likely due to its superior lubricating and anti-wear properties.

However, a markedly different trend is observed in figures 16(c) and (d), where the depth of cut is increased to 1.0 mm. Figure 16(c) reveals a rapid and severe increase in tool wear with decreasing cutting speed and increasing feed rate, especially at the higher feed rate when using pure palm oil is used as the cutting fluid. This implies that, while palm oil can slow tool degradation to some extent, it cannot totally avoid wear under high cutting loads. At these high working temperatures, thermal softening, oxidation, and chemical wear processes are anticipated to dominate, resulting in fast tool degradation.

In comparison, figure 16(d) illustrates that although tool wear also increases with decreasing cutting speed and increasing feed rate when using fly ash suspension, the overall wear is significantly lower than that observed

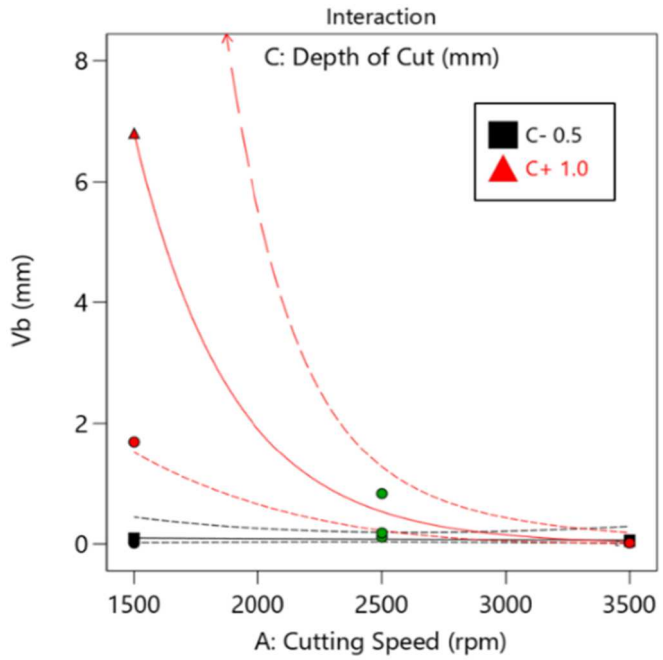

Figure 15. Interaction plot graph (a) Interaction plot of cutting speed and depth of cut (b) Interaction plot of cutting speed and type of cutting fluid towards tool wear.

with pure palm oil. The surface plot retains an upward slope, indicating notable wear at lower speeds and higher feeds. However, the presence of fly ash particles appears to mitigate the severity of tool degradation. This improvement can be attributed not only to the formation of a protective tribo-film but also to the enhanced thermal conductivity provided by the suspended fly ash particles, which facilitates more efficient heat dissipation during cutting [37]. Efficient heat transfer reduces the local temperature rise, minimizing thermal softening and maintaining tool hardness, especially at low cutting speeds and high feed rates where heat accumulation is more critical. This finding is consistent with the study by Sabri *et al* [38], where modified palm oils (MPOs) suspended with hybrid additives demonstrated superior thermal stability and oxidation resistance, further supporting the potential of particle-enhanced cutting fluids to improve machining performance under high thermal load conditions.

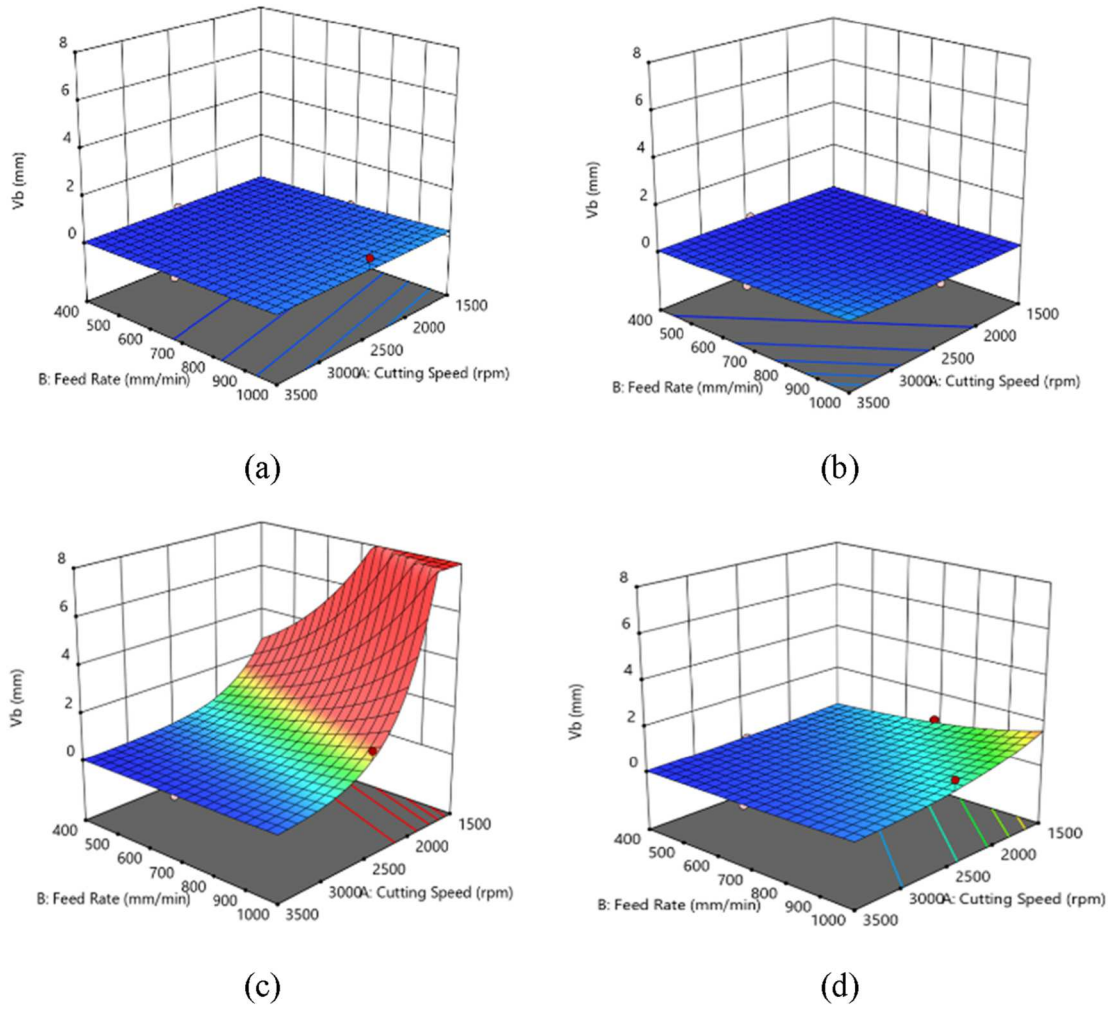

Figure 16. Response surface plot showing the interaction between cutting speed and feed rate on tool wear (a) palm oil at depth of cut of 0.5 mm (b) fly ash suspension at depth of cut of 0.5 mm (c) palm oil at depth of cut of 1.0 mm (d) fly ash suspension at depth of cut of 1.0 mm.

The overall results of tool wear indicate that fly-ash-based palm oil provides substantially better tool wear performance compared to pure palm oil, achieving up to a 70% reduction in flank wear under the tested cutting conditions. This trend agrees with the previous reports on hybrid nanofluids used for milling Inconel X-750, where hBN/Grpt nanofluid extended tool life significantly owing to improvement in heat dissipation and lubrication [39]. In the present work, the SiO_2-Al_2O_3-rich fly ash likely enhances thermal conductivity and contributes to the formation of a protective tribo-film, resulting in markedly lower wear compared to pure palm oil. These observations support broader conclusions from earlier studies that particle-enhanced lubricants, whether using engineered nanoparticles or waste-derived particles such as fly ash, can substantially improve tool life in sustainable machining applications.

Figure 17 shows the wear morphology of certain cutting tools under different cutting conditions. Figure 17 compares the flank wear morphology at mild cutting conditions (1500 rpm, 700 mm min^{-1}, 0.5 mm) under palm oil (Std 5) and fly ash suspension (Std 20). The tool machined with fly ash suspension (Std 20) exhibits the cleanest flank surface, with only light micro-scratches and no noticeable aluminium smearing (figure 17(a)). The cutting edges remained sharp with minimal wear, indicating that it was dominated by only mild abrasive action. In contrast, machining under palm oil condition (Std 5) produced clear evidence of adhesive wear, characterized by a smeared aluminium layer and the beginning of BUE formation along the nose area (figure 17(b)). Adhesive wear and shallow chipping marks indicate stronger tool-material interaction and higher friction where palm oil alone cannot transfer higher heat. These observations confirm that at low mechanical loads, the presence of fly ash particles significantly improves the cutting fluid quality by reducing adhesion and protecting the cutting edge, consistent with the lower Vb values recorded for Std 20, which is 0.008 mm.

On the other hand, a more pronounced difference was observed under different cutting conditions (cutting speed at 2500 rpm, feed rate at 1000 mm min^{-1}, and depth of cut 1.0 mm), as shown in the FESEM comparison

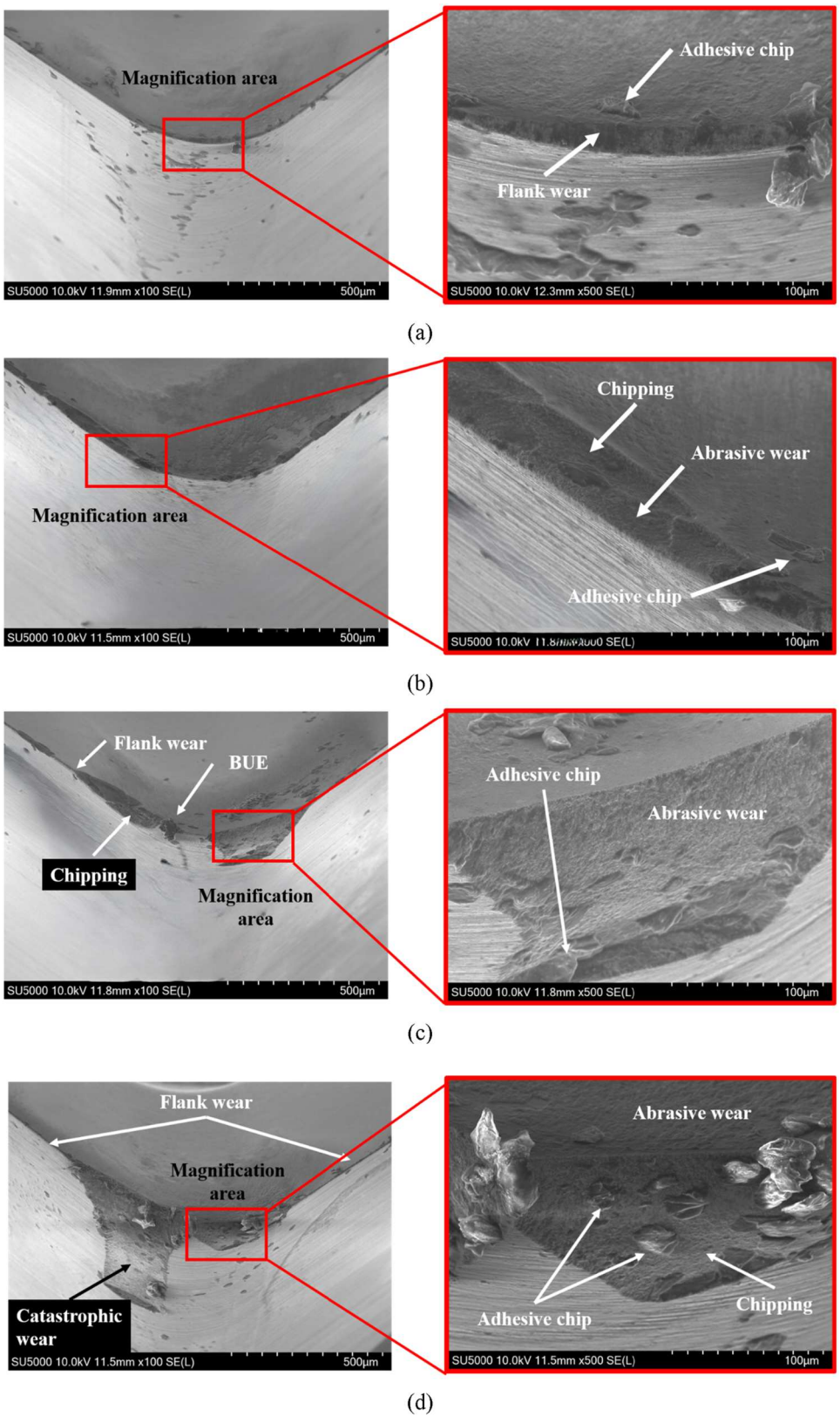

Figure 17. Tool-wear morphology patterns of the cutting tool under different working conditions (a) Std 20 (b) Std 5 (c) Std 27 and (d) Std 12.

between Std 27 and Std 12. The flank surface of Std 12 (palm oil) showed severe wear, including deep rough grooves, thicker chip adhesion, extensive smearing, and deeper chipping (figure 17(d)). In contrast, when using fly ash suspension, Std 27 showed a lower flank wear value under the same cutting parameters (figure 17(c)). Although rough chipping was present due to the higher feed and depth of cut, reduced chip adhesion was

Table 8. ANOVA for cutting force.

Source	Sum of squares	df	Mean square	F-value	p-value
Model	3792.33	4	948.08	8.65	0.0002
B-Feed Rate	454.46	1	454.46	4.14	0.0525
C-Depth of Cut	430.25	1	430.25	3.92	0.0587
D-Type of coolant	751.11	1	751.11	6.85	0.0148
CD	2156.50	1	2156.50	19.67	0.0002
Residual	2741.05	25	109.64		
Lack of Fit	2560.02	21	121.91	2.69	0.1736
Pure Error	181.03	4	45.26		
Cor Total	6533.38	29			

Table 9. Statistical summary of model for Fc.

R^2	Adjusted R^2	Predicted R^2	Adeq precision
0.5805	0.5133	0.3909	10.3513

observed. The lower tool damage indicated that the fly ash particles helped dissipate heat more effectively and formed a protective tribo-film even at high cutting loads, thus reducing the wear progression.

3.3. Cutting force

Table 8 shows the ANOVA analysis for the cutting force (resultant force). Based on the F-distribution table for $\alpha = 0.05$ with degrees of freedom $df_1 = 4$ and $df_2 = 25$, again, same as surface roughness, the critical F-value is approximately 2.76 [29]. Since the calculated F-value (8.65) is substantially greater than the critical value, the probability of observing such a large value due to noise is very low, confirming the adequacy and significance of the model. For cutting force, parameter D and interaction of CD are significant model terms. Although feed rate (B) and depth of cut (C) yield p-values slightly above 0.05 (0.0525 and 0.0587, respectively), their relatively high F-values indicate that they still exert a noticeable influence on the cutting force. Such behavior is common in machining responses, where interaction effects may dominate, as demonstrated by the strong CD interaction observed in this study.

The R^2 of the cutting force model is 0.5805 as shown in table 9, implying that 58.05% of the variability in cutting force is explained by the model. The adjusted R^2 of 0.5133 is close enough to the R^2, which confirms that unnecessary terms have not been included. The predicted R^2 of 0.3909 has a reasonable match with the adjusted R^2, reflecting an acceptable predictive capability of this response. The Adeq Precision of 10.3513 (>4) further confirms an adequate signal for the model and that it can be used to explore the design space effectively.

After removing insignificant factors, which is cutting speed, the response surface equation for MRR is shown in equation (4).

$$Fc = 45.66 - 5.33B + 5.19C - 5D - 11.61CD \quad (4)$$

The adequacy of the model is also supported by residual diagnostics for cutting force, presented in figures 18 to 20. The normal probability plot (figure 18) indicates that residuals are generally following a straight-line trend and, therefore, the normality assumption is met. The residuals-versus-run plot (figure 19) exhibits random scatter, which confirms that residuals are independent and free from drift. The residuals-versus-fitted plot (figure 20) reveals consistent scatter around the zero reference line, which suggests constant variance and no evidence of heteroscedasticity. Externally studentized residuals fall within Bonferroni limits (±3.54047), confirming that no outliers exist in this dataset.

Figure 21 illustrates the interaction plot between the type of cutting fluid and the depth of cut on cutting force. It is observed that cutting force increases steadily with increasing depth of cut when palm oil is used, reaching the highest value at 1.0 mm depth. In contrast, the fly ash suspension shows a relatively stable trend, with cutting force remaining lower and less sensitive to changes in depth of cut. This clearly indicates that the incorporation of fly ash particles enhances the lubricating efficiency of palm oil, thereby reducing the cutting resistance.

At lower depth of cut (0.5 mm), both fluids show comparable cutting force values. However, as the depth of cut increases, the difference becomes more significant. The cutting force associated with palm oil rises sharply, while fly ash suspension demonstrates a moderate reduction. This behaviour suggests that fly ash additives form protective tribo-films and improve load-carrying capacity, effectively minimizing friction and adhesion

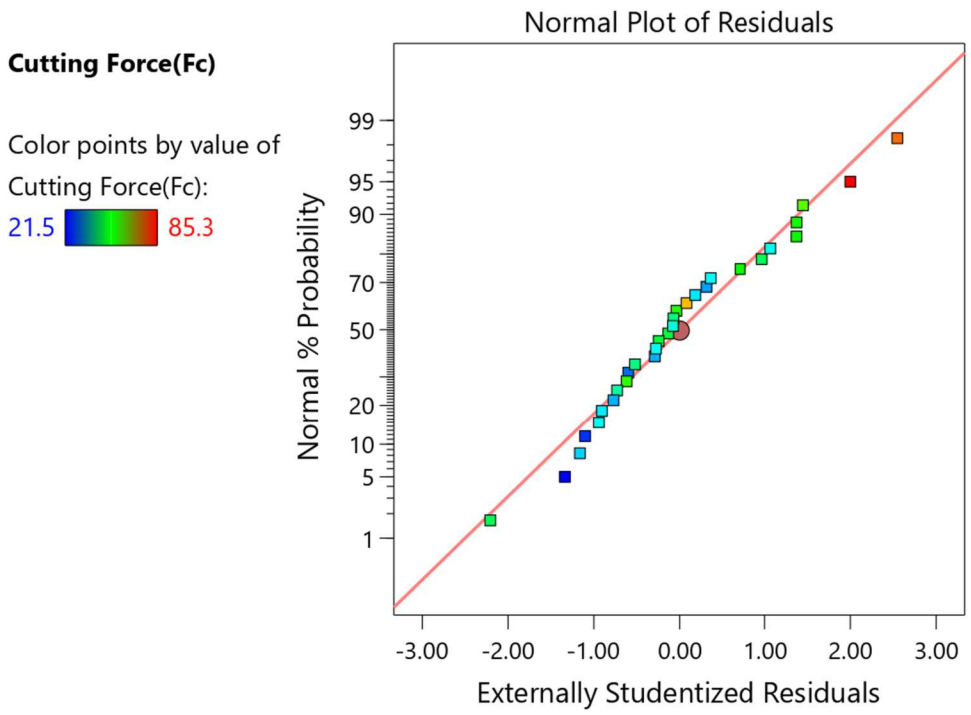

Figure 18. Normal probability plot for cutting force.

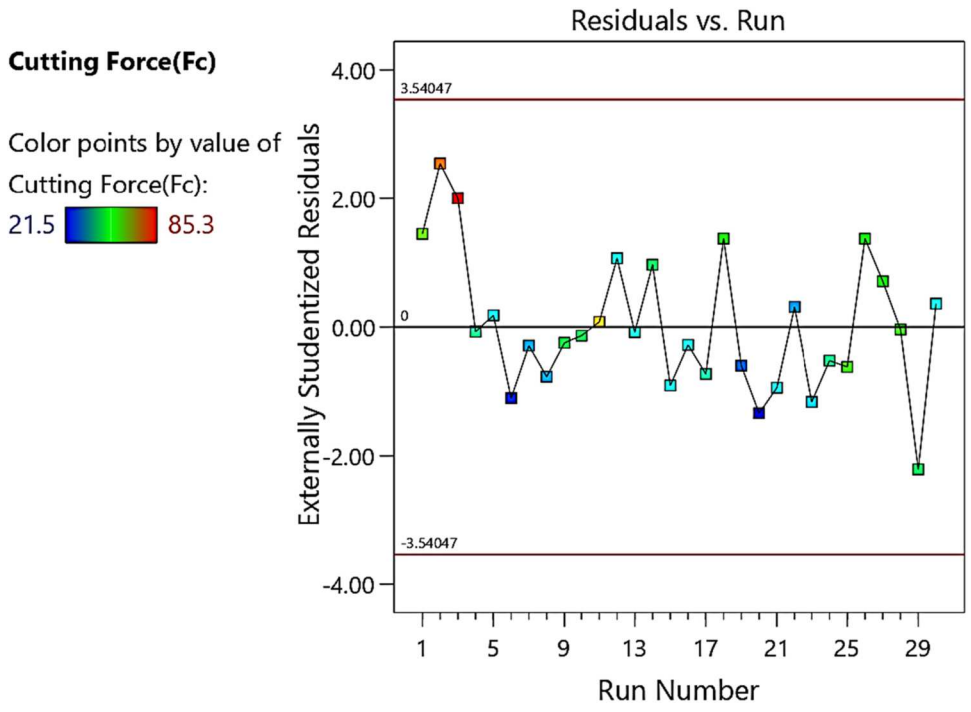

Figure 19. Residuals versus run for cutting force.

between the tool and workpiece. Similar findings have been reported in previous studies, where the addition of nanoparticles enhanced the thermal conductivity of nanocutting fluids, leading to more effective heat dissipation at the tool–chip interface and consequently lowering cutting forces [20]. In line with this, fly ash which can be classified as hybrid nanoparticles, has been reported to enhance particle dispersion and improve convective heat transfer due to its higher thermal conductivity, thereby further reducing cutting force under elevated cutting conditions [40]. Conversely, pure palm oil lacks such reinforcement, leading to higher friction and resistance under higher cutting loads.

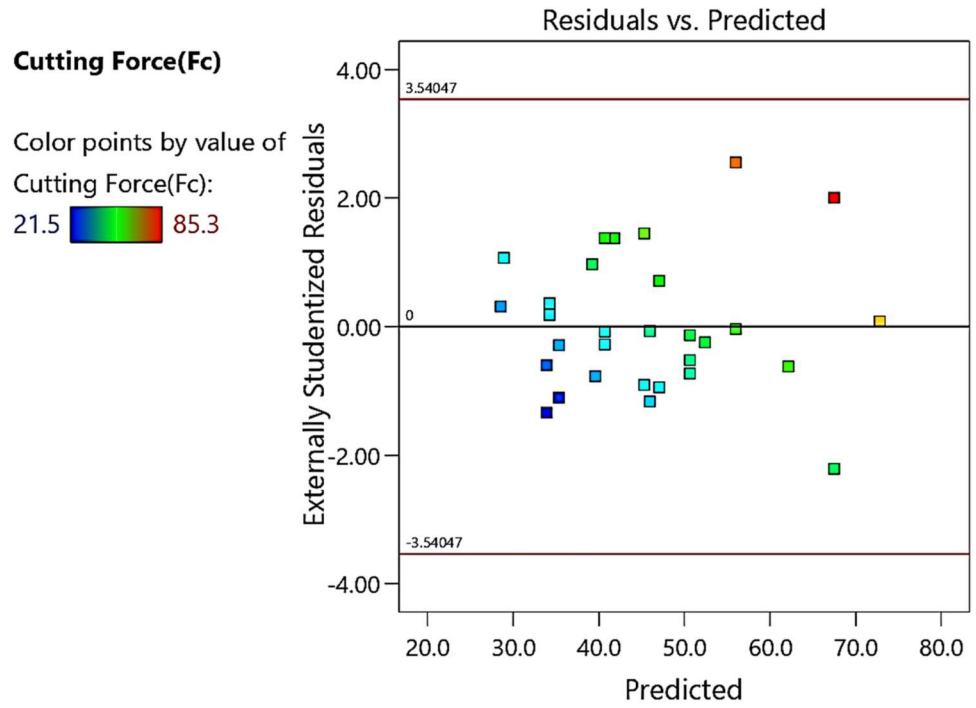

Figure 20. Residuals versus predicted values for cutting force.

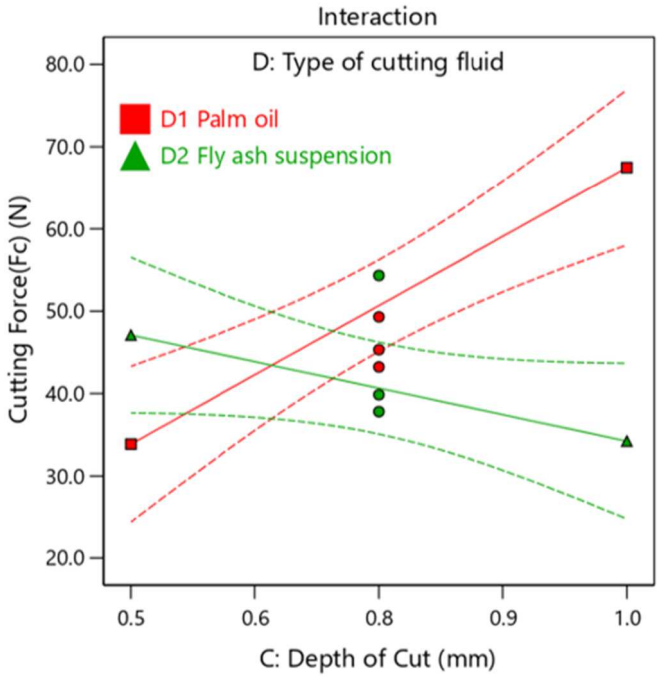

Figure 21. Response surface plot showing the interaction of type of cutting fluid and depth of cut towards cutting force.

The fly-ash suspension achieved a 19.75% reduction in cutting force, consistent with prior findings on nano-Al_2O_3-based MQL fluids, which similarly showed lower cutting forces due to improved wettability and thermal conductivity. A study conducted earlier on the development of nano-Al_2O_3 enriched coconut oil for machining AISI-1040 steel found that the addition of nanoparticles significantly improved the fluid's wettability, viscosity, and thermal conductivity, thereby reducing friction and subsequently cutting forces [41]. Although the machining parameters differ, both studies highlight the same governing mechanism. The presence of solid particles improves the fluid's spreading behaviour and enhances heat dissipation at the tool–chip

Table 10. ANOVA for MRR.

Source	Sum of squares	df	Mean square	F-value	p-value
Model	4.335E + 07	5	8.670E + 06	35.72	<0.0001
B-Feed Rate	3.255E + 07	1	3.255E + 07	134.14	<0.0001
C-Depth of Cut	6.250E + 06	1	6.250E + 06	25.75	<0.0001
D-Type of cutting fluid	1.318E + 06	1	1.318E + 06	5.43	0.0285
BD	1.507E + 06	1	1.507E + 06	6.21	0.0200
CD	1.719E + 06	1	1.719E + 06	7.08	0.0137
Residual	5.824E + 06	24	2.427E + 05		
Lack of Fit	5.421E + 06	20	2.710E + 05	2.69	0.1742
Pure Error	4.033E + 05	4	1.008E + 05		
Cor Total	4.917E + 07	29			

Table 11. Statistical summary of model for MRR.

R^2	Adjusted R^2	Predicted R^2	Adeq precision
0.8816	0.8569	0.8010	20.5260

interface, thereby reducing cutting resistance. This mechanism explains why fly ash maintains lower cutting forces at higher depths of cut compared to pure palm oil.

3.4. Material removal rate

Table 10 shows the ANOVA analysis for the MRR. According to Montgomery [29], F-distribution at a 95% confidence level ($\alpha = 0.05$) with degrees of freedom $df_1 = 5$ and $df_2 = 24$, the corresponding critical F-value is approximately 2.62. Because the calculated model F-value of 35.72 is substantially higher than this benchmark, it is highly unlikely that such a value could arise from random variation, thereby confirming the statistical significance and robustness of the model. For MRR, parameter B, C, D and interaction of BD and CD are significant model terms. Feed rate shows the highest F-value (134.14), confirming that it is the most dominant factor affecting MRR, followed by depth of cut and the cutting fluid-related interactions.

As shown in table 11, the MRR model exhibits strong statistical performance, with an R^2 value of 0.8816 indicating that 88.16% of the variation in MRR is explained by the process parameters. The adjusted R^2 value of 0.8569 and the predicted R^2 value of 0.8010 are in close agreement, confirming excellent model validity and predictive capability. Furthermore, the Adeq Precision value of 20.5260, which is substantially higher than the threshold of 4, demonstrates an excellent signal-to-noise ratio and confirms the robustness of the MRR model.

After removing insignificant factors, which is cutting speed, the response surface equation for MRR is shown in equation (5).

$$\text{MRR} = 3640.74 + 1426.39\ \text{B} + 625.00\ \text{C} + 209.63\ \text{D} + 306.94\ \text{BD} - 327.78\ \text{CD} \quad (5)$$

The diagnostic plots for MRR validate the accuracy of the developed model. The normal probability plot (figure 22) indicates that the residuals follow a linear trend, indicating that they are normally distributed. The residuals-versus-run plot (figure 23) exhibits a random, patternless scatter, suggesting independence of the residuals. Meanwhile, the residuals-versus-predicted plot (figure 24) shows the even fluctuation of the residuals around the zero-residual line, which also confirms homoscedasticity across fitted values. All observations are inside the Bonferroni-corrected limits of ±3.55968, hence no extreme values have been identified, proving the reliability of the developed model in relation to MRR.

Figure 25 shows response surface plot for the interaction between cutting speed and feed rate on MRR under different cutting fluids and depth of cut conditions. Figure 25(a) demonstrates that when using pure palm oil, the MRR remained low and was generally insensitive to cutting speed and feed rate, likely due to restricted chip thickness and poor load transfer. However, when using fly ash suspension (figure 25(b)), a modest increase in MRR was seen, attributed to improved lubrication and reduced friction, which facilitated slightly greater material removal even at low depths of cut.

Meanwhile, figure 25(c) depicts the scenario using palm oil lubrication at 1.0 mm depth of cut. The surface plot displays a strong positive gradient, especially when the feed rate increases, indicating that feed rate has a more pronounced influence on the MRR under these conditions. In comparison, figure 25(d) shows the most substantial increase in MRR among all situations. The surface plot for the combination of fly ash suspension and a 1.0 mm depth of cut reveals a clear and steep rise in MRR with increasing feed rate. This trend suggests

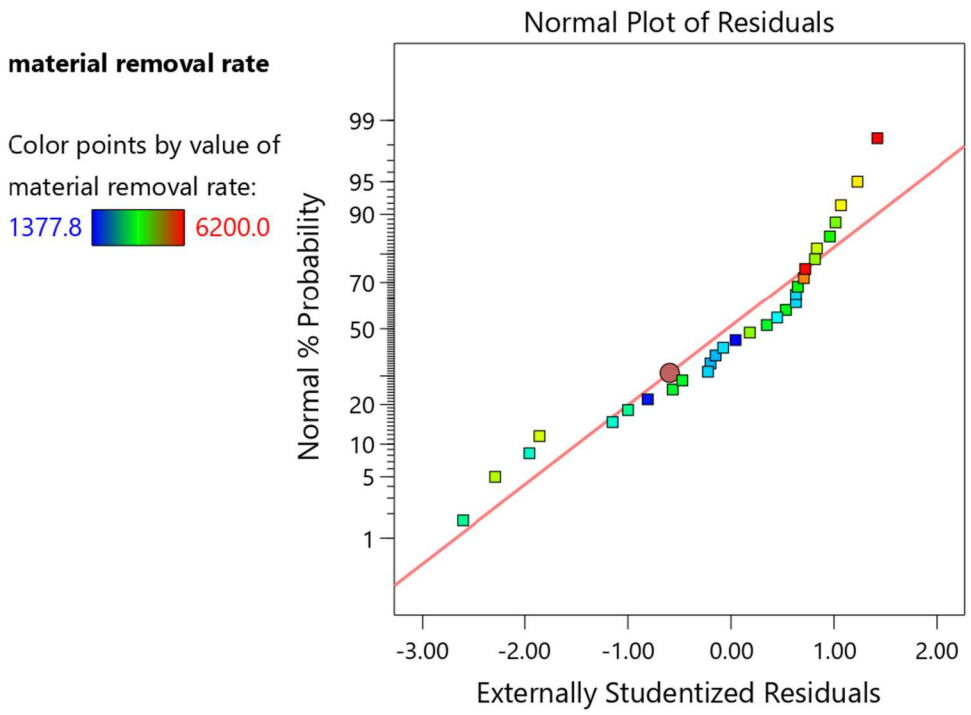

Figure 22. Normal probability plot for MRR.

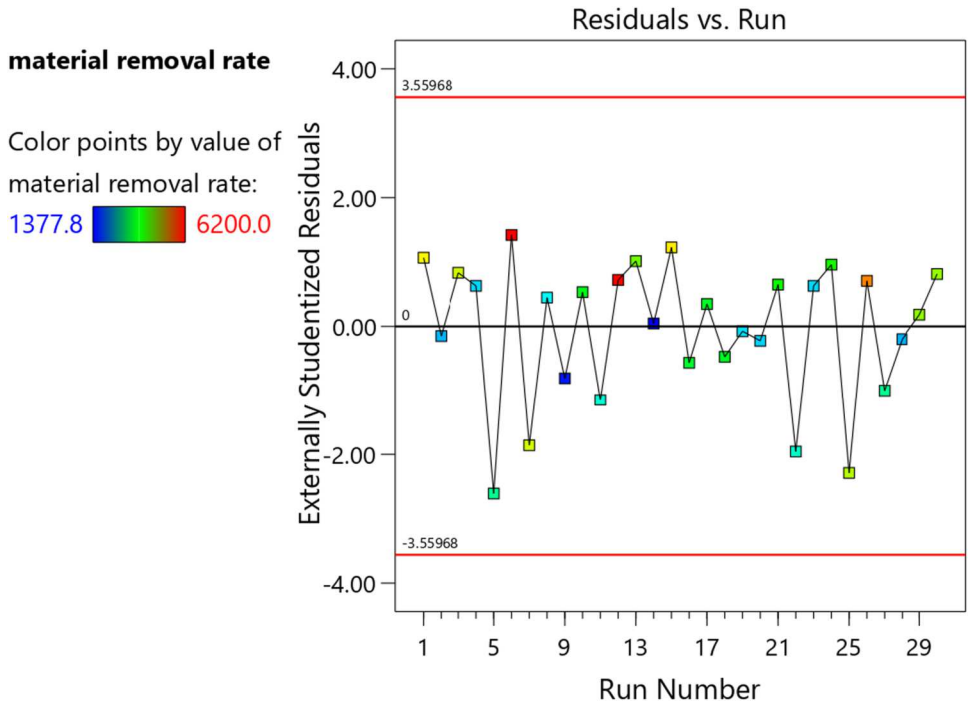

Figure 23. Residuals versus run for MRR.

that, under enhanced lubrication and more stable cutting conditions, higher feed rates contribute significantly to improved machining productivity. The inclusion of fly ash particles in the palm oil clearly plays an important role in decreasing friction, improving cooling, and maintaining tool sharpness, enabling more efficient material removal under extreme cutting conditions. These findings are consistent with those of Wang *et al* [42], who emphasized that while deeper cuts enhance material removal, they also demand effective lubrication strategies to mitigate tool wear and preserve surface integrity.

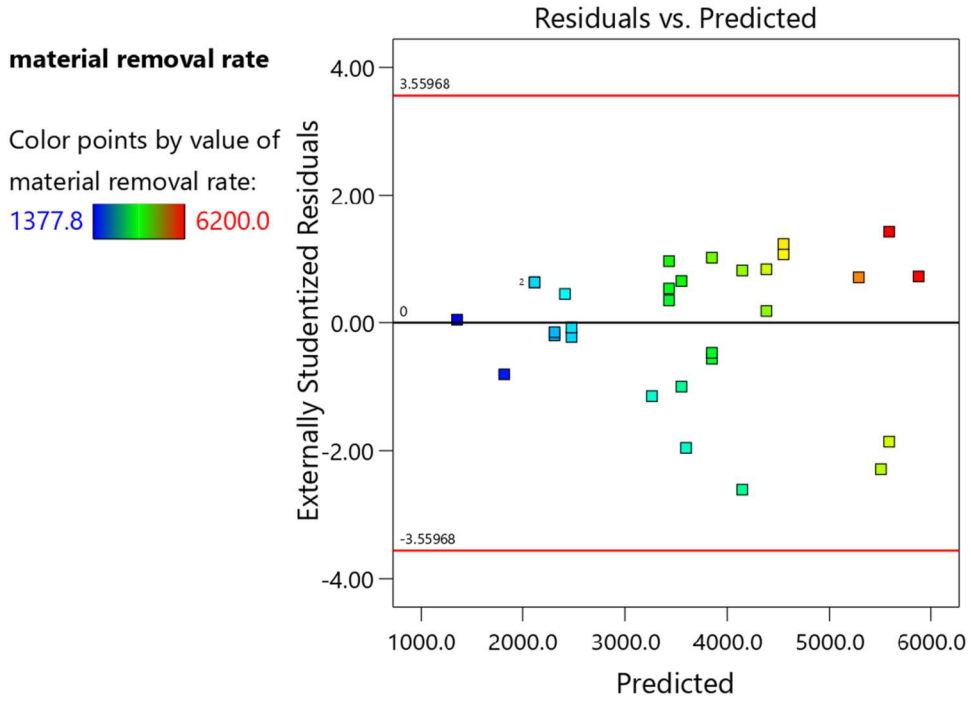

Figure 24. Residuals versus predicted values for MRR.

In this study, the addition of fly ash to palm oil led to a measurable increase in machining productivity, with the maximum MRR improving by 12% compared to pure palm oil. This improvement is attributed to the solid-lubricant behaviour of fly ash, whose SiO_2–Al_2O_3 rich particles contribute to friction reduction and chip formation stabilization. Once these solid particles enter the cutting zone, they act as micro-rolling and micro-burnishing agents that reduce shear deformation by decreasing the required energy input for chip removal. This leads to smoother chip flow, reduced tool–chip adhesion, and more continuous material removal, especially under high feed rates and larger depths of cut.

These observations are consistent with earlier particle-based MQL studies. For example, Jamil *et al* [43] reported that hybrid Al_2O_3–MWCNT nanofluids increased MRR during milling of Ti–6Al–4V by improving heat dissipation and reducing cutting resistance, achieving an optimal MRR of 303.9 $mm^3\ min^{-1}$ under enhanced lubrication conditions. Although the nanoparticle formulation and work material differ from those used in the present study, both works highlight the same underlying mechanism: suspended solid particles strengthen the lubricating film, improving heat transport and reducing chip–tool adhesion, thereby enabling higher material removal rates. Thus, the results of this work demonstrate that waste-derived fly ash can deliver comparable productivity gains to engineered nanoparticle-based MQL fluids.

3.5. Optimization parameter and validation run

The optimization analysis in this study focused primarily on minimizing surface roughness, tool wear and cutting force while maximize MRR. Table 12 shows the goal settings, weight assignments and importance levels used in the desirability-based multi-response optimization for cutting parameters and machining responses. From the table, the lower and upper weights were set at 1, which defines a linear desirability curve for each response. The importance levels were set to 5 for Ra and Vb, 4 for Fc and MRR, representing the need to prioritise surface integrity and tool life while still maintaining machining productivity. All input parameters (cutting speed, feed rate, depth of cut and type of cutting fluid) were kept 'in range' with equal importance (3). Based on the defined constraints and target responses, the Design-Expert software provided the predicted optimal combination of process parameters, as summarized in table 13.

To validate the proposed optimal parameters, a confirmation experiment was conducted in triplicate. The selected parameters were derived from the RSM optimization results, targeting the minimization of surface roughness, tool wear and cutting force while maximize MRR. The outcomes of the validation tests are summarized in table 14. As shown in table 14, the percentage errors between the experimental means and predicted values are 5.1% for Ra, 8.4% for Vb, 7.82% for Fc and 4.94% for MRR. These small deviations indicate a strong

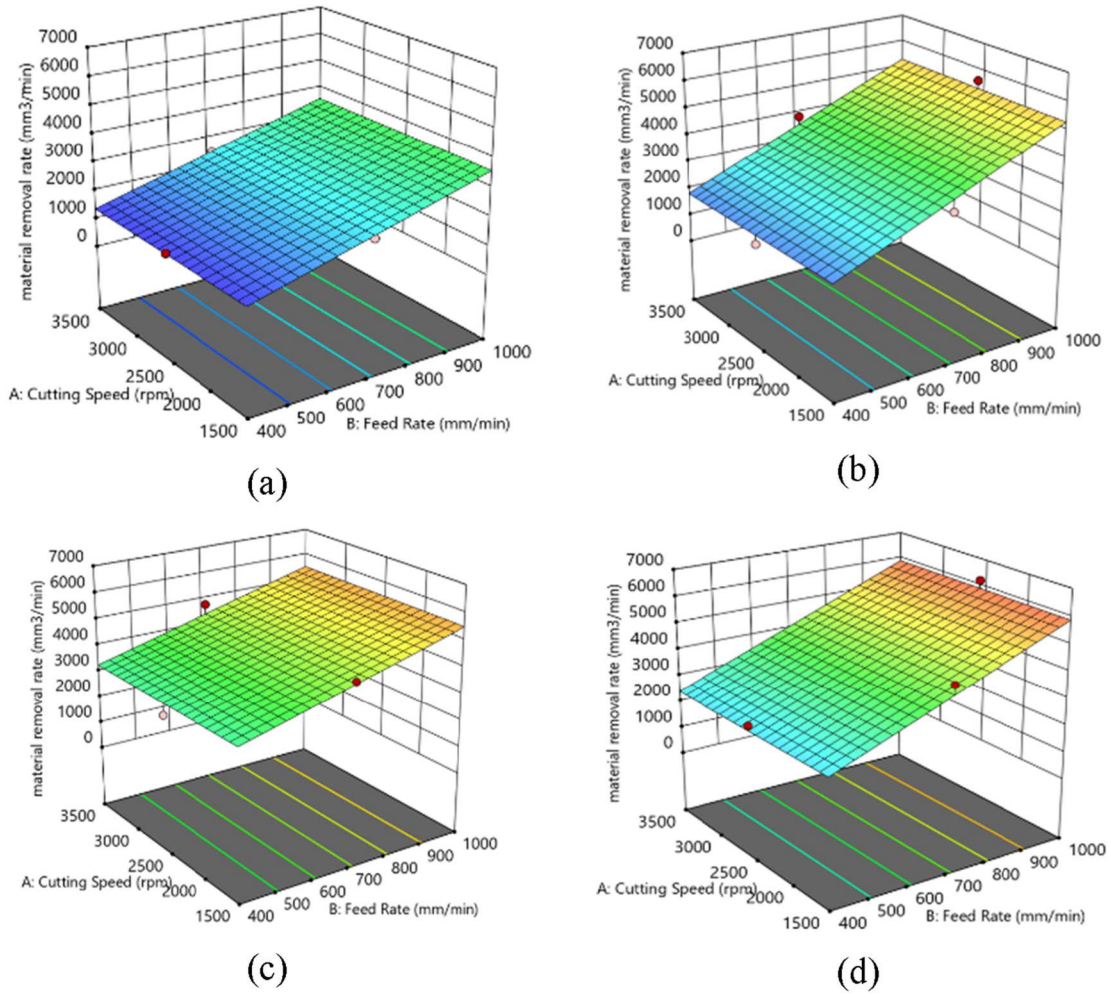

Figure 25. Response surface plot showing the interaction between cutting speed and feed rate on MRR (a) palm oil at depth of cut of 0.5 mm (b) fly ash suspension at depth of cut of 0.5 mm (c) palm oil at depth of cut of 1.0 mm (d) fly ash suspension oil at depth of cut of 1.0 mm.

Table 12. Desirability function settings for multi-response optimization.

Name	Goal	Lower limit	Upper limit	Lower weight	Upper weight	Importance
A: Cutting Speed	is in range	1500	3500	1	1	3
B: Feed Rate	is in range	400	1000	1	1	3
C: Depth of Cut	is in range	0.5	1	1	1	3
D: Type of cutting fluid	is in range	Palm oil	Fly ash suspension	1	1	3
Surface Roughness	minimize	0.19	1.825	1	1	5
Cutting Force	minimize	21.4744	85.2549	1	1	4
Flank wear	minimize	0.00738	1.74477	1	1	5
Material removal rate	maximize	1377.78	6200	1	1	4

Table 13. Predicted optimum milling parameter.

Cutting speed, rpm	Feed rate, mm/min	Depth of cut, mm	Type of cutting fluid	Ra, μm	Vb, mm	Fc, N	MRR, mm^3/min	Desirability
3500	840	1	Fly ash suspension	0.705	0.101	31.74	4959.9	0.718

agreement between the experimental and predicted results, thereby confirming the reliability of the optimized process parameters for achieving multi-objective performance improvements in the milling of aluminium alloy under MQL conditions.

Table 14. Results of confirmation test.

		Experimental				
Response	Predicted	1	2	3	Average	Error%
Ra	0.705	0.630	0.670	0.710	0.67	5.1
Vb	0.101	0.104	0.113	0.109	0.109	8.4
Fc	31.740	33.50	34.30	34.83	34.21	7.82
MRR	4959.9	4810.66	5210.66	5610.66	5210.66	4.94

4. Conclusions

This study comprehensively evaluated the effects of cutting speed, feed rate, depth of cut, and type of cutting fluid on the milling performance of aluminium alloy 6061 under MQL conditions. The analysis focused on surface roughness, tool wear, cutting force and MRR. The following conclusions can be drawn from the results:

(a) The incorporation of fly ash into palm oil significantly improved machining performance by reducing Ra, Vb and Fc while simultaneously increasing MRR, compared to the use of pure palm oil alone.

(b) Higher cutting speed resulted in reduced Ra, indicating smoother surface finishes. In contrast, Vb varied depending on the cutting fluid but generally remained low at elevated cutting speeds.

(c) Increasing the feed rate significantly improved the Fc and MRR but also accelerated tool wear and degraded Ra, particularly when palm oil was employed as the cutting fluid. A moderate feed rate range (400–700 mm min^{-1}) provided an optimal balance between tool life and surface quality.

(d) Depth of cut has a dominant effect on both tool wear and MRR. At 1.0 mm depth of cut, prominent Vb was observed, whereas lower depth of cut produced better surface quality and reduced tool wear.

(e) Cutting force was strongly influenced by both the type of cutting fluid and the depth of cut. Fly ash suspension consistently reduced cutting force across all cutting parameters. In contrast, palm oil resulted in higher cutting forces, particularly at larger depth of cut.

(f) The multi-objective optimization using RSM with BBD identified the optimal milling parameters for aluminium alloy 6061 as a cutting speed of 3500 rpm, feed rate of 840 mm min^{-1}, and depth of cut of 1.0 mm with fly ash suspension.

This study is limited to machining AL6061-T6 under selected MQL parameters, with the analysis focused on surface roughness, tool wear, cutting force, and material removal rate. Measurements such as cutting temperature, vibration, and detailed tool-wear mechanisms were not included. Future work will address these gaps by incorporating multi-sensor monitoring (e.g., temperature and vibration), detailed tool wear analysis, and investigation of additional aluminium alloys and cutting conditions. These extensions will provide a more comprehensive understanding of the underlying tribological and thermal phenomena under MQL-assisted machining.

Acknowledgments

This study is funded by Ministry of Higher Education (MOHE) of Malaysia through the Fundamental Research Grant Scheme (FRGS) No: FRGS/1/2023/TK10/UTEM/02/6. The authors would also like to thank Universiti Teknikal Malaysia Melaka (UTeM) for all the support.

Data availability statement

All data that support the findings of this study are included within the article (and any supplementary files).

Author contributions

Ainusyafiqah Shaaroni 0009-0005-7941-5181
Investigation (lead), Methodology (equal), Writing – original draft (lead)

Pay Jun Liew 0000-0001-6729-1576
Conceptualization (lead), Formal analysis (supporting), Writing – review & editing (supporting)

Raja Izamshah Raja Abdullah 0000-0002-1985-6736
Conceptualization (supporting), Data curation (supporting)

Kin Yuen Leong
Conceptualization (supporting), Formal analysis (supporting), Writing – review & editing (supporting)

Jingsi Wang 0000-0002-9390-9074
Resources (equal), Writing – review & editing (supporting)

References

[1] Rauf A, Khan M A, Jaffery S H I and Butt S I 2024 Effects of machining parameters, ultrasonic vibrations and cooling conditions on cutting forces and tool wear in meso scale ultrasonic vibrations assisted end-milling (UVAEM) of Ti–6Al–4V under dry, flooded, MQL and cryogenic environments–a statistical analysis *Journal of Materials Research and Technology* **30** 8287–303
[2] Fernando W L R, Sarmilan N, Wickramasinghe K C, Herath H M C M and Perera G I P 2020 Experimental investigation of minimum quantity lubrication (MQL) of coconut oil based metal working fluid *Mater. Today Proc.* **23** 23–6
[3] Korkmaz M E, Gupta M K, Ross N S and Sivalingam V 2023 Implementation of green cooling/lubrication strategies in metal cutting industries: a state of the art towards sustainable future and challenges *Sustain. Mater. Technol.* **36** e00641
[4] Kulkarni H B, Nadakatti M M, Patil M S and Kulkarni R M 2017 A review on nanofluids for machining *Current Nanoscience* **13** 634–53
[5] Geetha C H T S, Dash A K, Kavya B and Amrita M 2021 Analysis of hybrid nanofluids in machining AISI 4340 using minimum quantity lubrication *Mater. Today Proc.* **43** 579–86
[6] Nishad P K, Dubey V, Mishra D K and Sharma A K 2023 An investigation on performance of castor oil and Pongamia oil based cutting fluid in MQL milling of aluminium alloy 6061 *Mater. Today Proc.* (https://doi.org/10.1016/j.matpr.2023.05.305)
[7] Wang J, Yang X, Klemeš J ř J, Tian K, Ma T and Sunden B 2023 A review on nanofluid stability: preparation and application *Renew. Sustain. Energy Rev.* **188** 113854
[8] Shokrani A, Betts J and Carnevale M 2021 Thermal analysis in MQL end milling operations *Procedia CIRP* **101** 358–61
[9] Zhenjing D U A N, Changhe L I, Lan D O N G, Xiufang B A I, Min Y A N G, Dongzhou J I A, Runze L I, Huajun C A O and Xuefeng X U 2021 Milling surface roughness for 7050 aluminium alloy cavity influenced by nozzle position of nanofluid minimum quantity lubrication *Chin. J. Aeronaut.* **34** 33–53
[10] Ikhries I I and Al-Shawabkeh A F 2024 Novel methods for optimizing CNC aluminium alloy machining parameters in polymer mold cavities *International Journal of Lightweight Materials and Manufacture* **7** 507–19
[11] Cönger D B, Yapan Y F, Emiroğlu U ğ, Uysal A, E and Altan 2024 Influence of singular and dual MQL nozzles on sustainable milling of Al6061-T651 in different machining environments *J. Manuf. Processes* **109** 524–36
[12] Malik M A I, Kalam M A, Mujtaba M A and Almomani F 2023 A review of recent advances in the synthesis of environmentally friendly, sustainable, and nontoxic bio-lubricants: recommendations for the future implementations *Environ. Technol. Innov.* **32** 103366
[13] Luo X, Wu S, Wang D, Yun Y, An Q and Li C 2024 Sustainable development of cutting fluids: the comprehensive review of vegetable oil *J. Clean. Prod.* **473** 143544
[14] Owuna F J 2020 Stability of vegetable based oils used in the formulation of ecofriendly lubricants–a review *Egyptian Journal of Petroleum* **29** 251–6
[15] Selbmann E, Preiß M, Achour A B, Teicher U, Hänel A and Ihlenfeldt S 2022 Investigation of bio-based cooling lubricants for the machining of aircraft stainless steels *Procedia CIRP* **110** 47–52
[16] Kharka V, Mujumdar S and Shukla S 2023 Study on helical milling of SS 304 with small diameter tools under the influence of minimum quantity lubrication (MQL) *Manufacturing Letters* **35** 1312–7
[17] Durango-Giraldo G, Zapata-Hernandez C, Santa J F and Buitrago-Sierra R 2022 Palm oil as a biolubricant: literature review of processing parameters and tribological performance *J. Ind. Eng. Chem.* **107** 31–44
[18] Samylingam L *et al* 2024 Enhancing lubrication efficiency and wear resistance in mechanical systems through the application of nanofluids: a comprehensive review *Journal of Advanced Research in Micro and Nano Engineering* **16** 1–18
[19] Minh D T, Tran The L and Bao N T 2017 Performance of Al_2O_3 nanofluids in minimum quantity lubrication in hard milling of 60Si2Mn steel using cemented carbide tools *Advances in Mechanical Engineering* **9** 1687814017710618
[20] Gupta A, Kumar R, Kumar H, Mehta J S and Wadhwa A S 2024 Experimental study on the effect of combination ratio of Al_2O_3-MWCNT hybrid nano-cutting fluids while turning AISI 304 *Eng. Res. Express* **6** 045572
[21] Sen B, Mia M, Mandal U K and Mondal S P 2020 Synergistic effect of silica and pure palm oil on the machining performances of Inconel 690: a study for promoting minimum quantity nano doped-green lubricants *J. Clean. Prod.* **258** 120755
[22] Safiei W, Rahman M M, Yusoff A R, Arifin M N and Tasnim W 2021 Effects of SiO_2-Al_2O_3-ZrO_2 tri-hybrid nanofluids on surface roughness and cutting temperature in end milling process of aluminum alloy 6061-T6 using uncoated and coated cutting inserts with minimal quantity lubricant method *Arab. J. Sci. Eng.* **46** 7699–718
[23] Öztürk B and Kara F 2020 Calculation and estimation of surface roughness and energy consumption in milling of 6061 alloy *Adv. Mater. Sci. Eng.* **2020** 5687951
[24] Liew P J, Shaaroni A, Razak J, Kasim M S and Sulaiman M A 2017 Optimization of cutting condition in the turning of AISI D2 steel by using carbon nanofiber nanofluid *International Journal of Applied Engineering Research* **12** 2243–52 http://www.ripublication.com/ijaer17/ijaerv12n10_17.pdf
[25] Rafaizul N I A M, Rosli M A M, N, Salimen, Herawan S G and Hussain F 2024 Formulation of graphene nanoplatelets water-based nanofluids using polyvinylpyrrolidone (PVP) as surfactant *Journal of Advanced Research in Micro and Nano Engineering* **16** 35–47
[26] Jayakumar K 2024 Optimization of cutting force and surface roughness in end milling of AA-TiCp composite *Mater. Today Proc.* (https://doi.org/10.1016/j.matpr.2024.03.060)

[27] Ch R and Punna E 2024 Modelling and optimization of fabrication parameters for multi-walled carbon nanotubes-filled GFRP composites using RSM and Rao-1 algorithm *Eng. Res. Express* **6** 025554
[28] Khan M A 2025 Optimizing hybrid fiber concrete: an experimental analysis of steel and polypropylene fiber composites using RSM *Mater. Res. Express* **12** 025304
[29] Montgomery D C 2021 *Design and Analysis of Experiments* EMEA edition (Wiley)
[30] Anderson M J and Whitcomb P J 2017 *DOE Simplified: Practical Tools for Effective Experimentation* (CRC Press)
[31] Ping Z, Yue X, Shuangfeng H, Ailing S, Baoshun L and Xiao Y 2020 Experiment and simulation on the high-speed milling mechanism of aluminum alloy 7050-T7451 *Vacuum* **182** 109778
[32] Liew P J, Tay H S, Yap C Y, Othman I S, Raja R I and Tunggal D 2021 Tribological behaviour of palm oil mixed with fly ash microparticles as a bio-based lubricant for manufacturing processes. *Jurnal Tribologi* **31** 73–83 https://jurnaltribologi.mytribos.org/v31/JT-31-73-83.pdf
[33] Zadafiya K, Shah P, Shokrani A and Khanna N 2021 Recent advancements in nano-lubrication strategies for machining processes considering their health and environmental impacts *J. Manuf. Processes* **68** 481–511
[34] Liew P J, Shaaroni A, Sidik N A C and Yan J 2017 An overview of current status of cutting fluids and cooling techniques of turning hard steel *Int. J. Heat Mass. Transfer.* **114** 380–94
[35] Bhushan R K 2023 Impact of SiC particle size and weight% on tool life while machining of AA7075/SiC composite *Journal of Alloys and Metallurgical Systems* **3** 100016
[36] Bee P H, SeshaTalpa Sai P H V, Devaraj S, Chaitanya Lahari M L R, Sharma K V and Narayanaswamy K S 2023 Effect of copper nano-cutting fluids in end milling of al 6061 and its influence on work piece morphology *Mater. Today Proc.* (https://doi.org/10.1016/j.matpr.2023.02.425)
[37] Liew P J, Shaaroni A, Razak J A, Hadzley M and Bakar A 2018 Comparison between carbon nanofiber (CNF) nanofluid with deionized water on tool life and surface roughness in turning of D2 steel *Journal of Advanced Research Fluid Mechanics and Thermal Sciences* **46** 169–74 https://akademiabaru.com/doc/ARFMTSV46_N1_P169_174.pdf
[38] Sabri A M, Talib N, Karim Z A, Sani A S A, Kamdani K, Kunar S and Sani N 2024 Physical characterization of modified palm oil with hybrid additives nanofluids. *Journal of Advanced Research in Micro and Nano Engineering* **15** 41–51
[39] Şirin Ş and Kıvak T 2021 Effects of hybrid nanofluids on machining performance in MQL-milling of Inconel X-750 superalloy *J. Manuf. Processes* **70** 163–76
[40] Tota R K, Nagaraju D, Syed J and Mohammad A R 2025 Performance of heat transfer in Al_2O_3/MWCNT hybrid nanofluid flow using machine learning models *Eng. Res. Express* **7** 015528
[41] Tiwari S, Amarnath M and Gupta M K 2023 Synthesis, characterization, and application of Al_2O_3/coconut oil-based nanofl42uids in sustainable machining of AISI 1040 steel *J. Mol. Liq.* **386** 122465
[42] Wang B, Liu Z, Cai Y, Luo X, Ma H, Song Q and Xiong Z 2021 Advancements in material removal mechanism and surface integrity of high speed metal cutting: a review *Int. J. Mach. Tools Manuf* **166** 103744
[43] Jamil M, Khan A M, Hegab H, Gupta M K, Mia M, He N, Zhao G, Song Q and Liu Z 2020 Milling of Ti–6Al–4V under hybrid Al_2O_3-MWCNT nanofluids considering energy consumption, surface quality, and tool wear: a sustainable machining *Int. J. Adv. Manuf. Technol.* **107** 4141–57